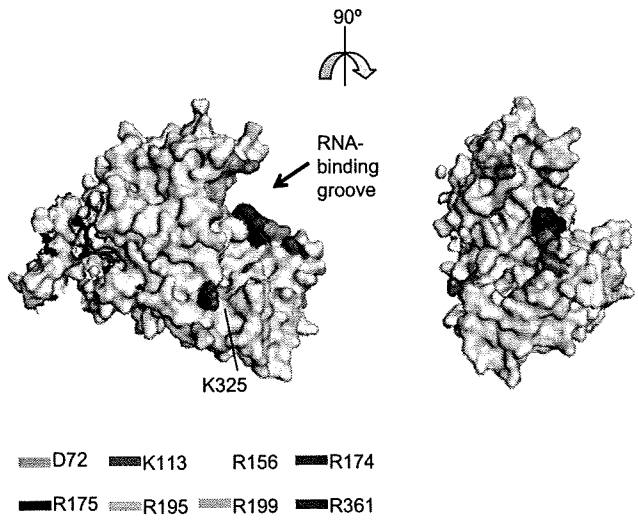

FIG. 4. Crystal structure of influenza A virus NP. The images were created with the program PYMOL (W. L. Delane; http://www.pymol.org), and the NP structure was obtained from the Protein Data Bank (41) (accession number 2IQH). The locations of the amino acid residues that affect the efficient incorporation of multiple vRNA segments into VLPs are shown in color.

through the interaction of RNPs and/or other essential host cellular components, leading to the efficient incorporation of the eight vRNA segments into virus particles.

Influenza A virus NP has at least two NLS sequences. An unconventional NLS is located between residues 3 and 13 and is responsible for NP binding to karyopherins α1 and α2 (35). The second NLS is a bipartite signal located in the middle of NP (residues 198 to 216) (37). The bipartite NLS can function as an NLS to a limited extent when it is fused to a cytoplasmic reporter protein (37). Its contribution to NP nuclear import, however, is not as significant as that of NLS1 (37). In this study, we attempted to generate five viruses that possessed amino acid substitutions in the bipartite NLS (R199A, R208A, R213A, R214A, and R216A). The R208A and R213A mutant viruses were not recoverable because these mutations significantly reduced viral transcription, consistent with a previous report that the bipartite NLS was essential for vRNA transcription (31). In contrast, the single amino acid substitution R214A or R216A had no effect on viral-genome replication/transcription, NP localization, or virus replication. These results suggest that a single mutation at position 214 or 216 of NP may not be sufficient to affect NP function, although multiple amino acid changes in the bipartite NLS (positions 213, 214, and 216) completely disrupt vRNA transcription, NP nuclear accumulation, and virus replication (31). We also found that a mutation at position 199 did not affect viral-genome replication/transcription and NP nuclear transport.

In this study, we found that mutations A337R, E339A, Q405A, S407A, F412A, V414A, R416A, F488A, F489A, D491A, and E495A significantly decreased the transcription of influenza vRNA (Table 1). The crystal structure of influenza NP shows that each NP contains a tail loop, formed by residues 402 to 428 (41). This tail loop is inserted into the body domain of a neighboring molecule in a counterclockwise direction when viewed along the threefold axis from the side of the head domain. Mutagenesis revealed that the tail loop is essential for NP oligomerization, which in turn is necessary for vRNA transcription (8, 42). Since the mutations we tested (A337R, E339A, Q405A, S407A, F412A, V414A, R416A, F488A, F489A, D491A, and E495A) reside in or near the NP-NP-interacting region (8, 41), they may disrupt the NP-NP interaction, leading to inhibition of viral-genome replication and transcription.

Using coimmunoprecipitation, Biswas et al. showed that coexpression of the components of the polymerase protein complex (PB1, PB2, or PA) with NP either together or pairwise revealed that NP interacts with PB1 and PB2 but not with PA (3). These experiments implicated three NP regions—amino acids 1 to 160, 256 to 340, and 340 to 498—in binding to the PB2 subunit of the viral polymerase (3, 33). In our study, mutant viruses R150A, E254A, A260R, K273A, A337A, E339A, R355A, A387R, Q405A, F412A, R416A, F488A, and F489A were not viable, and their abilities to support vRNA transcription were decreased significantly. Our results suggest that these NP mutations (i.e., R150A, E254A, A260R, K273A, A337A, E339A, R355A, A387R, Q405A, F412A, R416A, F488A, and F489A, which lie in or near the PB2 binding domain) block the interaction of NP with the polymerase subunits (PB1 and PB2), leading to defective viral growth.

In summary, we have identified amino acids that alter the functionality of NP in viral-genome replication/transcription. We have also identified amino acids in NP that facilitate efficient incorporation of multiple vRNA segments into progeny virions, suggesting a role of these amino acid residues in the assembly of influenza A virus segments in the form of RNPs. Further analyses of the significance of NP should provide information essential to our understanding of influenza virus replication.

ACKNOWLEDGMENTS

We thank Susan Watson for editing the manuscript and Krisna Wells and Martha McGregor for excellent technical assistance. We also thank Bill Sudgen for kindly providing plasmids.

This work was supported in part by U.S. National Institute of Allergy and Infectious Diseases Public Health Service research grants, by a grant-in-aid for Specially Promoted Research, and by a contract research fund for the Program of Funding Research Centers for Emerging and Reemerging Infectious Diseases from the Ministry of Education, Culture, Sports, Science and Technology; by ERATO (Japan Science and Technology Agency); and by grants-in-aid from the Ministry of Health, Labor, and Welfare of Japan.

REFERENCES

1. **Albo, C., A. Valencia, and A. Portela.** 1995. Identification of an RNA binding region within the N-terminal third of the influenza A virus nucleoprotein. J. Virol. **69**:3799–3806.
2. **Avalos, R. T., Z. Yu, and D. P. Nayak.** 1997. Association of influenza virus NP and M1 proteins with cellular cytoskeletal elements in influenza virus-infected cells. J. Virol. **71**:2947–2958.
3. **Biswas, S. K., P. L. Boutz, and D. P. Nayak.** 1998. Influenza virus nucleoprotein interacts with influenza virus polymerase proteins. J. Virol. **72**:5493–5501.
4. **Deng, T., O. G. Engelhardt, B. Thomas, A. V. Akoulitchev, G. G. Brownlee, and E. Fodor.** 2006. Role of Ran binding protein 5 in nuclear import and assembly of the influenza virus RNA polymerase complex. J. Virol. **80**: 11911–11919.
5. **Digard, P., D. Elton, K. Bishop, E. Medcalf, A. Weeds, and B. Pope.** 1999. Modulation of nuclear localization of the influenza virus nucleoprotein through interaction with actin filaments. J. Virol. **73**:2222–2231.
6. **Dos Santos Afonso, E., N. Escriou, I. Leclercq, S. van der Werf, and N. Naffakh.** 2005. The generation of recombinant influenza A viruses expressing a PB2 fusion protein requires the conservation of a packaging signal overlapping the coding and noncoding regions at the 5′ end of the PB2 segment. Virology **341**:34–46.

7. **Duhaut, S. D., and J. W. McCauley.** 1996. Defective RNAs inhibit the assembly of influenza virus genome segments in a segment-specific manner. Virology **216**:326–337.
8. **Elton, D., L. Medcalf, K. Bishop, D. Harrison, and P. Digard.** 1999. Identification of amino acid residues of influenza virus nucleoprotein essential for RNA binding. J. Virol. **73**:7357–7367.
9. **Elton, D., M. Simpson-Holley, K. Archer, L. Medcalf, R. Hallam, J. McCauley, and P. Digard.** 2001. Interaction of the influenza virus nucleoprotein with the cellular CRM1-mediated nuclear export pathway. J. Virol. **75**:408–419.
10. **Enami, M., G. Sharma, C. Benham, and P. Palese.** 1991. An influenza virus containing nine different RNA segments. Virology **185**:291–298.
11. **Fujii, K., Y. Fujii, T. Noda, Y. Muramoto, T. Watanabe, A. Takada, H. Goto, T. Horimoto, and Y. Kawaoka.** 2005. Importance of both the coding and the segment-specific noncoding regions of the influenza A virus NS segment for its efficient incorporation into virions. J. Virol. **79**:3766–3774.
12. **Fujii, Y., H. Goto, T. Watanabe, T. Yoshida, and Y. Kawaoka.** 2003. Selective incorporation of influenza virus RNA segments into virions. Proc. Natl. Acad. Sci. USA **100**:2002–2007.
13. **Gog, J. R., S. Afonso Edos, R. M. Dalton, I. Leclercq, L. Tiley, D. Elton, J. C. von Kirchbach, N. Naffakh, N. Escriou, and P. Digard.** 2007. Codon conservation in the influenza A virus genome defines RNA packaging signals. Nucleic Acids Res. **35**:1897–1907.
14. **Honda, A., K. Ueda, K. Nagata, and A. Ishihama.** 1988. RNA polymerase of influenza virus: role of NP in RNA chain elongation. J. Biochem. **104**:1021–1026.
15. **Huang, T. S., P. Palese, and M. Krystal.** 1990. Determination of influenza virus proteins required for genome replication. J. Virol. **64**:5669–5673.
16. **Katz, J. M., M. Wang, and R. G. Webster.** 1990. Direct sequencing of the HA gene of influenza (H3N2) virus in original clinical samples reveals sequence identity with mammalian cell-grown virus. J. Virol. **64**:1808–1811.
17. **Kennedy, G., and B. Sugden.** 2003. EBNA-1, a bifunctional transcriptional activator. Mol. Cell. Biol. **23**:6901–6908.
18. **Kobasa, D., M. E. Rodgers, K. Wells, and Y. Kawaoka.** 1997. Neuraminidase hemadsorption activity, conserved in avian influenza A viruses, does not influence viral replication in ducks. J. Virol. **71**:6706–6713.
19. **Kobayashi, M., T. Toyoda, D. M. Adyshev, Y. Azuma, and A. Ishihama.** 1994. Molecular dissection of influenza virus nucleoprotein: deletion mapping of the RNA binding domain. J. Virol. **68**:8433–8436.
20. **Liang, Y., Y. Hong, and T. G. Parslow.** 2005. *cis*-Acting packaging signals in the influenza virus PB1, PB2, and PA genomic RNA segments. J. Virol. **79**:10348–10355.
21. **Marsh, G. A., R. Hatami, and P. Palese.** 2007. Specific residues of the influenza A virus hemagglutinin viral RNA are important for efficient packaging into budding virions. J. Virol. **81**:9727–9736.
22. **Martin, K., and A. Helenius.** 1991. Nuclear transport of influenza virus ribonucleoproteins: the viral matrix protein (M1) promotes export and inhibits import. Cell **67**:117–130.
23. **Mena, I., E. Jambrina, C. Albo, B. Perales, J. Ortin, M. Arrese, D. Vallejo, and A. Portela.** 1999. Mutational analysis of influenza A virus nucleoprotein: identification of mutations that affect RNA replication. J. Virol. **73**:1186–1194.
24. **Neumann, G., T. Watanabe, H. Ito, S. Watanabe, H. Goto, P. Gao, M. Hughes, D. R. Perez, R. Donis, E. Hoffmann, G. Hobom, and Y. Kawaoka.** 1999. Generation of influenza A viruses entirely from cloned cDNAs. Proc. Natl. Acad. Sci. USA **96**:9345–9350.
25. **Niwa, H., K. Yamamura, and J. Miyazaki.** 1991. Efficient selection for high-expression transfectants with a novel eukaryotic vector. Gene **108**:193–199.
26. **Noda, T., H. Sagara, A. Yen, A. Takada, H. Kida, R. H. Cheng, and Y. Kawaoka.** 2006. Architecture of ribonucleoprotein complexes in influenza A virus particles. Nature **439**:490–492.
27. **Noton, S. L., E. Medcalf, D. Fisher, A. E. Mullin, D. Elton, and P. Digard.** 2007. Identification of the domains of the influenza A virus M1 matrix protein required for NP binding, oligomerization and incorporation into virions. J. Gen. Virol. **88**:2280–2290.
28. **Odagiri, T., and M. Tashiro.** 1997. Segment-specific noncoding sequences of the influenza virus genome RNA are involved in the specific competition between defective interfering RNA and its progenitor RNA segment at the virion assembly step. J. Virol. **71**:2138–2145.
29. **O'Neill, R. E., J. Talon, and P. Palese.** 1998. The influenza virus NEP (NS2 protein) mediates the nuclear export of viral ribonucleoproteins. EMBO J. **17**:288–296.
30. **Onishi, M., S. Kinoshita, Y. Morikawa, A. Shibuya, J. Phillips, L. L. Lanier, D. M. Gorman, G. P. Nolan, A. Miyajima, and T. Kitamura.** 1996. Applications of retrovirus-mediated expression cloning. Exp. Hematol. **24**:324–329.
31. **Ozawa, M., K. Fujii, Y. Muramoto, S. Yamada, S. Yamayoshi, A. Takada, H. Goto, T. Horimoto, and Y. Kawaoka.** 2007. Contributions of two nuclear localization signals of influenza A virus nucleoprotein to viral replication. J. Virol. **81**:30–41.
32. **Parvin, J. D., P. Palese, A. Honda, A. Ishihama, and M. Krystal.** 1989. Promoter analysis of influenza virus RNA polymerase. J. Virol. **63**:5142–5152.
33. **Portela, A., and P. Digard.** 2002. The influenza virus nucleoprotein: a multifunctional RNA-binding protein pivotal to virus replication. J. Gen. Virol. **83**:723–734.
34. **Stegmann, T., J. M. White, and A. Helenius.** 1990. Intermediates in influenza induced membrane fusion. EMBO J. **9**:4231–4241.
35. **Wang, P., P. Palese, and R. E. O'Neill.** 1997. The NPI-1/NPI-3 (karyopherin alpha) binding site on the influenza a virus nucleoprotein NP is a nonconventional nuclear localization signal. J. Virol. **71**:1850–1856.
36. **Watanabe, T., S. Watanabe, T. Noda, Y. Fujii, and Y. Kawaoka.** 2003. Exploitation of nucleic acid packaging signals to generate a novel influenza virus-based vector stably expressing two foreign genes. J. Virol. **77**:10575–10583.
37. **Weber, F., G. Kochs, S. Gruber, and O. Haller.** 1998. A classical bipartite nuclear localization signal on Thogoto and influenza A virus nucleoproteins. Virology **250**:9–18.
38. **Whittaker, G., M. Bui, and A. Helenius.** 1996. Nuclear trafficking of influenza virus ribonucleoproteins in heterokaryons. J. Virol. **70**:2743–2756.
39. **Wright, P. F., G. Neumann, and Y. Kawaoka.** 2007. Orthomyxoviruses, p. 1691–1740. *In* D. M. Knipe, P. M. Howley, D. E. Griffin, R. A. Lamb, M. A. Martin, B. Roizman, and S. E. Straus (ed.), Fields virology, 5th ed. Lippincott Williams & Wilkins, Philadelphia, PA.
40. **Yasuda, J., S. Nakada, A. Kato, T. Toyoda, and A. Ishihama.** 1993. Molecular assembly of influenza virus: association of the NS2 protein with virion matrix. Virology **196**:249–255.
41. **Ye, Q., R. M. Krug, and Y. J. Tao.** 2006. The mechanism by which influenza A virus nucleoprotein forms oligomers and binds RNA. Nature **444**:1078–1082.
42. **Ye, Z., T. Liu, D. P. Offringa, J. McInnis, and R. A. Levandowski.** 1999. Association of influenza virus matrix protein with ribonucleoproteins. J. Virol. **73**:7467–7473.

JOURNAL OF VIROLOGY, July 2009, p. 6429–6434 Vol. 83, No. 13
0022-538X/09/$08.00+0 doi:10.1128/JVI.00293-09

RuvB-Like Protein 2 Is a Suppressor of Influenza A Virus Polymerases▽

Satoshi Kakugawa,[1] Masayuki Shimojima,[1] Gabriele Neumann,[2] Hideo Goto,[1] and Yoshihiro Kawaoka[1,2,3,4]*

Division of Virology, Department of Microbiology and Immunology, Institute of Medical Science, University of Tokyo, 4-6-1 Shirokaneda, Minato-ku, Tokyo 108-8639, Japan[1]; Department of Pathobiological Sciences, School of Veterinary Medicine, University of Wisconsin, Madison, Wisconsin 53706[2]; Exploratory Research for Advanced Technology, Japan Science and Technology Agency, Saitama 332-0012, Japan[3]; and International Research Center for Infectious Diseases, Institute of Medical Science, University of Tokyo, Tokyo 108-8639, Japan[4]

Received 10 February 2009/Accepted 6 April 2009

In pro- and eukaryotic cells, RuvB-like protein 2 (RBL2) resolves Holliday junction recombination intermediates. Here, we identified RBL2 as a suppressor of influenza A virus replication. Human RBL2 appears to interfere with the oligomerization of the viral nucleoprotein, a critical step in the assembly of viral replication complexes.

Influenza A virus is an enveloped virus that belongs to the *Orthomyxoviridae* family and contains eight negative-sense RNA segments encoding 10 to 11 proteins (16). The RNA polymerase complex consists of three subunits, PB1, PB2, and PA. These polymerase subunits and nucleoprotein (NP), together with the viral RNA (vRNA), form the viral ribonucleoprotein complex (vRNP), which is the minimum component for vRNA replication and transcription.

Although some host factors have now been identified that interact with viral proteins (reviewed in reference 14), relatively little is known about the interplay between virus and host factors. We therefore developed a screening system to identify host proteins in a functional assay. Of the candidates that we identified that regulate virus RNA synthesis, RuvB-like protein 2 (RBL2) was identified as an inhibitor of vRNA synthesis.

RBL proteins (RBL1 and RBL2) are members of the AAA+ (ATPases associated with diverse cellular activities) family of helicases. They share moderate homology with bacterial RuvB, the ATP-dependent motor of the RuvAB complex that drives branch migration of the holiday junction (4). RBL1 and RBL2 are essential for viability in *Saccharomyces cerevisiae* and *Drosophila melanogaster* and may have similarly important roles in humans (1, 10).

In mammalian cells, the RBL proteins modulate cellular transformation, signaling, apoptosis, and the response to DNA damage by interacting with proteins such as β-catenin, c-Myc, and ATF2 (1, 2, 21). Moreover, they modulate rRNA processing and small nucleolar RNA maturation (12, 20) and function in complexes such as the chromatin remodeling complex INO80 (18) and the histone acetylase Tip60 complex (9).

Here, we provide evidence that RBL2 inhibits influenza virus replication. The protein interacts with the viral NP protein and interrupts its oligomerization, leading to inhibition of viral polymerase activity.

* Corresponding author. Mailing address: International Research Center for Infectious Diseases, Institute of Medical Science, University of Tokyo, Tokyo 108-8639, Japan. Phone: 81 3 5449 5310. Fax: 81 3 5449 5408. E-mail: kawaoka@ims.u-tokyo.ac.jp.

▽ Published ahead of print on 15 April 2009.

MATERIALS AND METHODS

Cell culture and viruses. Human embryonic kidney cells (293T cells and 293 cells) were cultured in Dulbecco's modified Eagle's medium (Sigma) supplemented with 10% heat-inactivated fetal calf serum and antibiotics. QT6 quail fibrosarcoma cells were maintained in Ham's F12K medium (MP Biomedicals) supplemented with 10% fetal calf serum and 10% tryptose phosphate broth (Sigma). Madin-Darby canine kidney (MDCK) cells were cultured in minimal essential medium containing 5% newborn calf serum and antibiotics. A/WSN/33 virus ([WSN] H1N1) was generated by reverse genetics (15) and propagated in MDCK cells. Viruses were titrated by plaque assay in MDCK cells.

Plasmids. The PB1, PB2, PA, and NP proteins of the A/Hong Kong/483/97 virus ([HK483] H5N1) were expressed using the pCAGGS vector (7) for the library screen. For all other experiments, these genes were derived from the WSN strain. The three polymerase cDNAs from the WSN strain fused to a c-Myc tag sequence at the 3′ termini and the NP cDNA from the WSN strain fused to a c-Myc tag sequence at the 5′ terminus were also inserted into pCAGGS. pPolI-GFP (where PolI is polymerase I and GFP is green fluorescent protein) drives the synthesis of negative-sense vRNAs comprising the 3′ noncoding region of the neuraminidase (HK483) vRNA, the complementary coding sequence of enhanced GFP (EGFP), and the 5′ noncoding region of the neuraminidase vRNA. Similarly, PolI-Luc drives the transcription of a virus-like RNA expressing luciferase.

Quail RBL2 (qRBL2) was cloned from QT6 cells by using the 5′ RACE System (Invitrogen) according to the manufacturer's instructions. Human RBL2 and RBL1 (hRBL2 and hRBL1, respectively) were cloned from human 293T cells. Briefly, RNA was extracted from these cells by use of an RNeasy Mini Kit (Qiagen). Reverse transcription-PCR (RT-PCR) was performed using an oligo(dT) primer, followed by PCR with gene-specific primers. hRBL2-DN (D299N) (2), which is designed to inactivate helicase activity, was constructed by using site-directed mutagenesis. These PCR products were cloned into the pCAGGS vector and then sequenced.

To assess the interaction between hRBL2 and the viral polymerase in living cells, we used a CoralHue Fluo-Chase kit (Amalgaam). Using the vectors in this kit, we constructed plasmids for the expression of the three polymerases, NP, and hRBL2 fused with the N- or C-terminal portion of Kusabira-Green, resulting in GN and GC fusion proteins (for example, pPB1-GN or pPB1-GC).

Library screening. Human embryonic kidney 293T cells were transfected with HK483 polymerase and NP protein expression plasmids (note that PB2 possesses glutamic acid at position 627), with a plasmid for the synthesis of a virus-like RNA encoding EGFP (PolI-EGFP) and with the quail QT6 cDNA library. Cells were incubated for 2 days at 33°C and collected, and GFP-expressing cells were sorted by a FACSCalibur instrument (BD). Plasmid DNA was then extracted from the cells and amplified in *Escherichia coli*. Cells that expressed high levels of GFP underwent selection three times, at which point their plasmid DNA was extracted and sequenced.

Luciferase assay. Luciferase assays were performed by use of a dual-luciferase reporter assay system (Promega) on a microplate luminometer (Veritas; Turner Biosystems, Sunnyvale, CA), according to the manufacturer's instructions. The

internal control for the dual-luciferase assay was pGL4.74(hRluc/TK) (Promega).

Analysis of virus propagation. To establish virus growth rates, three wells of 293 cells were transfected with the respective plasmid or small interfering RNA (siRNA) and 24 h (plasmid) or 48 h (siRNA) later infected with WSN at a multiplicity of infection (MOI) of 0.05. The cells were maintained at 37°C. At various time points, supernatants were assayed for virus titers by plaque assay in MDCK cells.

Knockdown of hRBL2 by use of siRNA. siRNA specific to RBL2 (catalog no. HSS116737) was purchased from Invitrogen. At 48 h posttransfection with the siRNA, cells were tested for RBL2 expression levels by Western blot analysis.

Quantification of vRNA products. To assess viral polymerase activity, cells transfected with protein expression plasmids or siRNAs were infected with WSN at an MOI of 2. At various time points, cells were washed three times with phosphate-buffered saline, after which the RNA was extracted and subjected to RT-PCR with NP gene-specific primers (sequences will be provided upon request) or oligo(dT) primers. The resultant cDNAs were quantified with LightCycler, version 2.0 (Roche), by NP gene-specific primers; beta-actin-specific primers served as an internal control.

Western blot analysis. To assess hRBL2 expression levels, cells transfected with the respective hRBL2 protein expression plasmid were suspended in Tris-glycine–sodium dodecyl sulfate (SDS) sample buffer (Invitrogen) and subjected to Western blot analysis with anti-hRBL2 (BD Transduction Laboratories) and anti-beta-actin (as an internal control; Sigma) antibodies, according to the manufacturer's instructions. Biotinylated anti-mouse immunoglobulin G (IgG) antibody (Vector) was used as a secondary antibody. Bands were detected using a Vectastain ABC kit (Vector) and ECL Plus Western Blotting Detection Reagents (GE Healthcare); the VersaDoc Imaging System (Bio-Rad) was used to quantify band intensities.

To analyze the expression of the viral M1 protein, cells transfected with protein expression plasmids or siRNA were infected with WSN at an MOI of 3 and incubated at 37°C. At the time points indicated in Fig. 2C or 3C, the cells were washed three times with phosphate-buffered saline and resuspended in Tris-glycine–SDS sample buffer. Western blot analysis was then performed with monoclonal antibodies specific to the M1 protein; beta-actin served as a control. Biotinylated anti-mouse IgG antibody (Vector) was used as a secondary antibody. Bands were detected as described above.

To assess the interaction of hRBL2 with viral polymerase complexes, 293T cells were transfected with plasmids for the expression of hRBL2 (pChRBL2), the viral polymerase proteins (pCAGGS-PB1, -PB2, and -PA), Myc-tagged NP protein, and, in a subset of experiments, a plasmid for the synthesis of virus-like RNA (PolI-GFP). Twenty-four hours later, Myc-tagged proteins were immunoprecipitated with anti-c-Myc agarose (Sigma). Nontagged NP served as a negative control. The beads were resuspended in Tris-glycine–SDS sample buffer, and Western blot analysis was performed with an antibody specific for hRBL2. Biotinylated anti-mouse IgG antibody (Vector) was used as a secondary antibody. Bands were detected as described above.

To assess the interaction of hRBL2 with individual components of the replication machinery, pChRBL2 was cotransfected with plasmids for the synthesis of Myc-tagged polymerase and NP proteins (pCPB1-Myc, pCPB2-Myc, pCPA-Myc, or pCMyc-NP). Immunoprecipitations were performed as described above.

BiFC assays. To examine the interaction of hRBL2 with viral proteins in living cells, we performed bimolecular fluorescence complementation (BiFC) assays using a CoralHue Fluo-Chase kit (Amalgaam). Briefly, the respective proteins were fused to N- or C-terminal portions of Kusabira-Green, resulting in GN or GC fusion proteins. Pairs of GN and GC fusion proteins were transfected into 293T cells and subjected 12 or 24 h later to luciferase assays or fluorescence-activated cell sorting (FACS) analysis, respectively.

RESULTS AND DISCUSSION

To identify host proteins that regulate viral replication, we developed a screening system in which human embryonic kidney 293T cells are transfected with a plasmid for the synthesis of a virus-like RNA encoding EGFP (PolI-EGFP) and with plasmids for the expression of the influenza A virus polymerase and NP proteins (Fig. 1). The PB2 protein possesses glutamic acid at position 627, which attenuates replication in mammalian systems at 33°C but allows efficient replication in avian systems (19). To identify avian host factors that rescue efficient

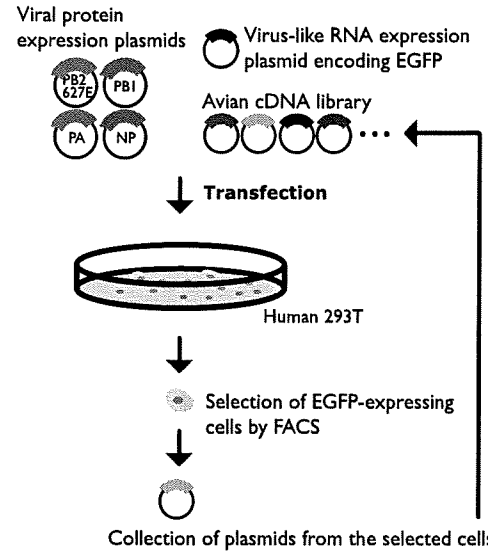

FIG. 1. Identification of cellular proteins that enhance influenza virus replication. Cells were transfected with plasmids encoding the HK483 (H5N1) PB2, PB1, PA, and NP proteins (the PB2 protein possesses glutamic acid at position 627; PB2-627E). Cells were cotransfected with PolI-EGFP for the synthesis of a virus-like RNA and with an avian (quail cell) cDNA expression library. Cells expressing avian proteins that support efficient replication by PB2-627E in mammalian cells at 33°C produce increased amounts of EGFP. GFP-expressing cells were selected by a FACS cell sorter. After three rounds of selection, plasmid DNA was extracted from the cells and sequenced.

replication, we cotransfected cells with a cDNA expression library derived from quail QT6 cells. Cells were incubated for 2 days at 33°C, and then GFP-expressing cells were sorted by FACSCalibur (BD). After three rounds of selection, we extracted plasmid DNAs and sequenced them. Among the quail proteins that upregulated viral replication was a truncated qRBL2 protein that lacked 217 N-terminal amino acids (ΔN-qRBL2).

A role for RBL proteins in the regulation of viral infections has not been described to date. However, using a genome-wide RNA interference screen in *Drosophila* to identify host genes important for influenza virus replication, we found that knockdown of the *Drosophila* homolog of hRBL2 enhanced reporter gene expression of the influenza virus replicon (6). In addition, Mayer et al. identified hRBL2 as a cellular interaction partner of influenza vRNPs (13). However, neither Hao et al. nor Mayer et al. assessed the biological significance of the RBL2 interaction with influenza vRNPs.

To confirm that ΔN-qRBL2 affects influenza virus RNA replication, we expressed it in human embryonic kidney (293) cells that also expressed the polymerase and NP proteins and a virus-like RNA encoding luciferase. Viral polymerase activity was indeed upregulated upon expression of ΔN-qRBL2 (Fig. 2A). We then overexpressed the full-length hRBL2 and qRBL2 in 293 cells that were subsequently infected with influenza virus strain WSN (H1N1) at an MOI of 1. Assessment of vRNA, cRNA, and mRNA levels by real-time RT-PCR at 3 h postinfection revealed downregulation of polymerase activity upon overexpression of hRBL2 or qRBL2 (Fig. 2B). As a consequence, viral protein synthesis (Fig. 2C) and replication

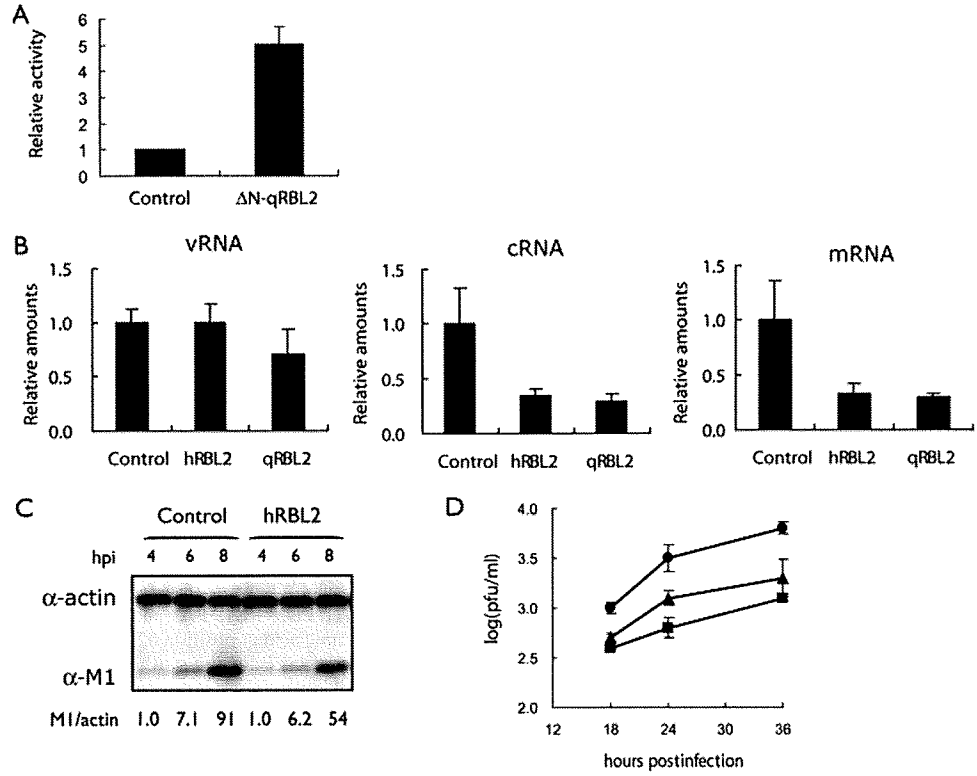

FIG. 2. Effect of RBL2 expression on influenza virus replication and growth. (A) ΔN-qRBL2 increases influenza virus replication in a minireplicon assay. 293T cells were transfected with plasmids expressing HK483 PB1, PB2-627K, PA, and NP proteins, pPolI-Luc, and ΔN-qRBL2. Twenty-four hours after incubation at 33°C, luciferase expression was detected. (B) Viral polymerase activity in cells expressing hRBL2 or qRBL2. 293 cells were transfected with plasmids expressing qRBL2 or hRBL2 or a control vector. Twenty-four hours later, cells were infected with strain WSN (MOI of 1). Three hours later, RNA was extracted and quantified by real-time RT-PCR with primer sets specific for NP vRNA, cRNA, or mRNA. These values were normalized to beta-actin. The error bars represent standard deviations (n = 3). (C) Viral M1 protein production in cells overexpressing hRBL2. 293 cells expressing hRBL2 or a control vector were infected with strain WSN (MOI of 3). At the indicated hours postinfection (hpi), cell lysates were subjected to Western blot analysis with antibodies against M1 and beta-actin. The values show the ratio of M1 to actin normalized to control cells 4 h after infection. (D) Influenza virus titers in 293 cells overexpressing hRBL2 or qRBL2. 293 cells overexpressing hRBL2 (square), qRBL2 (triangle), or a control vector (circle) were infected with strain WSN (MOI of 0.05). The cells were incubated at 37°C for the indicated time periods. Virus titers in the supernatant were determined by plaque assays in MDCK cells. The error bars represent standard deviations (n = 3). α, anti.

(Fig. 2D) were restricted. These findings indicate that ΔN-qRBL2 (identified in our screen) likely enhances influenza virus replication by acting as a dominant negative protein that competes with the endogenous RBL2 and that RBL2 is a general rather than host-species-specific host factor that suppresses influenza virus replication.

To further demonstrate that RBL2 interferes with influenza virus replication, we knocked it down in 293 cells by use of a specific siRNA (Fig. 3A, left and middle lanes). In these cells, the amounts of viral transcripts were increased relative to control cells (Fig. 3B, compare white and black bars), an effect that was partially reversed upon transfection of RBL2 siRNA-treated cells with a plasmid expressing hRBL2 (pChRBL2) (Fig. 3A, right lane, and B). Further, viral protein production and replication increased in RBL2 siRNA-treated cells (Fig. 3C and D), demonstrating that hRBL2 has an antiviral effect on influenza virus replication.

RBL2 possesses ATPase activity, which is critical for its biological function (2, 4). We therefore assessed a dominant negative form of RBL2 that lacks ATPase activity (hRBL2-DN) (2) for its effects on influenza virus growth. We found that hRBL2-DN interfered with polymerase activity and virus growth at almost the same level as the wild-type protein (data not shown). Hence, the ATPase activity of hRBL2 is not critical for its antiviral effect.

To investigate the interaction of hRBL2 with influenza vRNPs, we expressed hRBL2, the three polymerase subunits, and c-Myc-tagged NP protein in the absence or presence of a virus-like RNA. hRBL2 interacted with the viral replication complex regardless of the presence of vRNA (Fig. 4A). To assess which viral protein interacts with hRBL2, c-Myc-tagged polymerase and NP proteins were separately expressed with hRBL2 and immunoprecipitated with beads coated with an anti-c-Myc antibody. Interestingly, Western blot analysis showed that hRBL2 interacts with three different vRNP components—NP, PB2, and PB1 (Fig. 4B).

To further study the interaction of hRBL2 with vRNP components, we used a BiFC assay (8, 11) in which the proteins of interest were fused to N-terminal and C-terminal portions of Kusabira-Green (resulting in GN and GC fusion proteins, respectively); interaction of the proteins of interest thus resulted in Kusabira-Green fluorescence (Fig. 5A, upper panel). Strong

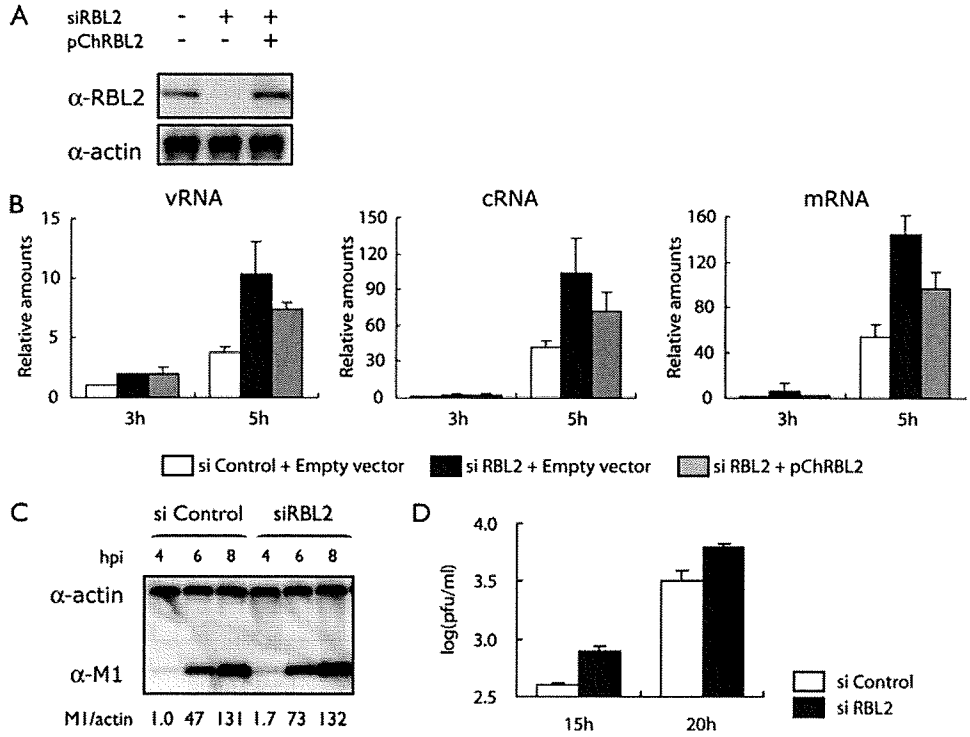

FIG. 3. Effect of hRBL2 knockdown on influenza virus replication. (A) Knockdown of hRBL2 in 293 cells. 293 cells were transfected with an siRNA specific to hRBL2 (siRBL2) or with a nonspecific control siRNA. Cells were also transfected with a plasmid expressing hRBL2 (pChRBL2) or a control vector. Two days later, hRBL2 expression levels were assessed by Western blot analysis. Beta-actin expression levels served as an internal control. (B) Viral polymerase activity in cells treated with an siRNA to hRBL2. 293 cells were transfected with hRBL2-specific or control siRNAs (si Control) and incubated at 37°C for 48 h. The transfected cells were then infected with strain WSN (MOI of 1). The amounts of vRNA, cRNA, and mRNA were determined at 5 h postinfection as described in the legend of Fig. 2b. (C) Viral M1 protein production in hRBL2 knockdown cells and control cells. Cells were transfected with siRNAs as described above and infected with WSN virus at an MOI of 3. M1 protein levels were assessed as described in the legend of Fig. 2c. (D) Influenza virus titers in hRBL2 knockdown cells and control cells. Cells were treated with siRNAs as described above, infected with WSN virus at an MOI of 0.05, and incubated at 37°C for the indicated time periods. Virus titers were determined in MDCK cells. The error bars represent standard deviations (n = 3). α, anti.

fluorescence was detected for the hRBL2 interaction with NP (Fig. 5A), whereas the level of fluorescence suggested no interaction or only moderate interaction of hRBL2 and the polymerase proteins in this assay.

NP was found to interact with hRBL2 in both the immunoprecipitation and BiFC assays. To assess if hRBL2 interferes with NP oligomerization, which is important for its biological activities (3, 22), we tested the NP-NP interaction in cells

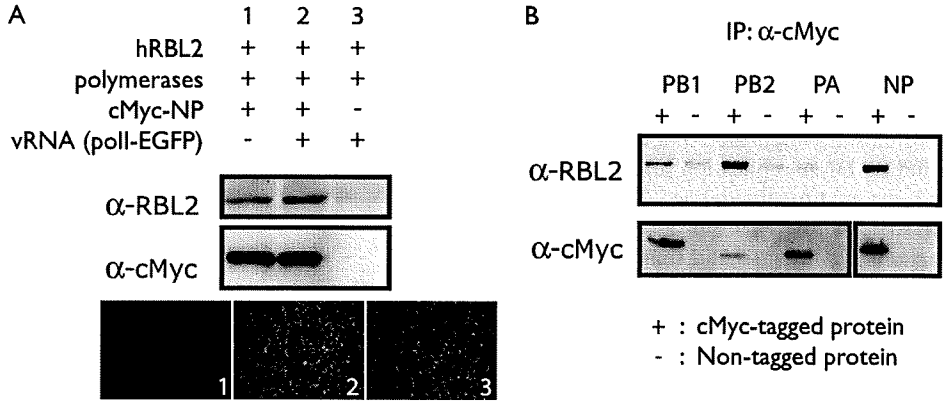

FIG. 4. Interaction of hRBL2 with viral proteins. (A) hRBL2 interacts with viral RNP complexes. The three viral polymerase proteins and c-Myc-tagged NP were expressed in 293T cells in the absence or presence of virus-like RNA (lanes 1 and 2). Nontagged NP was expressed as a negative control (lane 3). One day later, cell lysates were immunoprecipitated with anti-c-Myc beads. Western blot analysis was carried out with anti-hRBL2 and anti-c-Myc antibodies. EGFP expression in transfected cells indicates the functionality of c-Myc-tagged NP protein. (B) hRBL2 interacts with NP, PB2, and PB1. The three polymerase and NP proteins were individually tested for their interaction with hRBL2 as described above. α, anti; IP, immunoprecipitation.

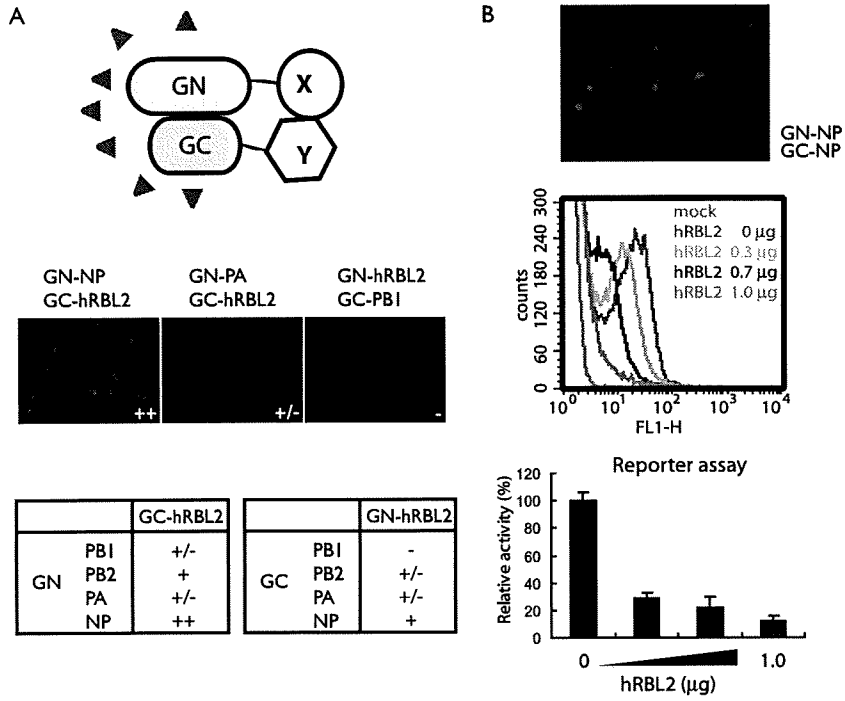

FIG. 5. hRBL2 interferes with NP oligomerization. (A) BiFC assay to assess interactions between hRBL2 and vRNP components. The proteins of interest were fused to the N- or C-terminal portions of Kusabira-Green (GN or GC). Interaction between the proteins of interest thus results in fluorescence. hRBL2 interacts with NP but not with the polymerase subunits. (B) hRBL2 inhibits NP oligomerization in a dose-dependent manner. Cells were transfected with plasmids for the expression of PB2, PB1, PA, pPolI-GFP, and GN-NP and GC-NP. NP-NP interaction was detected by microscopy and FACS analysis (middle panel, red curve). This interaction decreased with increasing amounts of hRBL2 (middle panel). Reporter gene expression in transfected cells indicates the functionality of the GN-NP and GC-NP fusion proteins and the biological significance of hRBL2 interference with NP oligomerization.

overexpressing hRBL2. As expected, we detected NP-NP interaction in the BiFC assay (Fig. 5B, upper panel); however, hRBL2 overexpression decreased the levels of fluorescence (indicative of NP-NP interaction) in a dose-dependent manner (Fig. 5B, middle panel). Similarly, reporter gene expression from a virus-like RNA was also reduced by hRBL2 expression in a dose-dependent manner (Fig. 5B, lower panel), demonstrating the functionality of NP fusion products and the biological significance of the hRBL2 interference with NP oligomerization. Collectively, these data suggest that hRBL2 disrupts the proper assembly of NP oligomers and, thereby, interrupts its biological activities. In addition to identifying this new host antiviral mechanism, our study also suggests RBL2 as a promising target for antiviral drug development.

Mammalian RBL proteins are implicated in a wide range of cellular activities, including DNA replication and repair, cell cycle progression, and chromatin remodeling (4). Structural analysis revealed that RBL2 and RBL1 can assemble into a double hexameric ring complex in vitro and that the dodecamer is likely one of the functional forms of the proteins (5, 17). Currently, it is not clear whether one of the hexamers contains exclusively RBL2 and the other RBL1 or whether both contain equimolar amounts of RBL2 and RBL1 (4). However, each protein is thought to have specific roles, and some data suggest subunit-specific functions that may not require RBL1/RBL2 complex formation (4). This is in line with findings by Mayer et al., who identified hRBL2, but not hRBL1, as a cellular interaction partner of vRNPs (13). Moreover, we did not detect a role for hRBL1 in influenza virus infection (data not shown). Hence, the inhibitory effect of hRBL2 on influenza virus seems to be a specific function of RBL2 rather than of the RBL1/RBL2 heterooligomer.

ACKNOWLEDGMENTS

We thank Susan Watson for editing the manuscript. We also thank H. Mimuro and N. Ishijima for technical support.

This research was supported by a Grant-in-Aid for Specially Promoted Research from the Ministry of Education, Culture, Sports, Science, and Technology of Japan; by a Grant-in-Aid for JSPS Fellows from the Japanese Society for the Promotion of Science (JSPS); by ERATO (Japan Science and Technology Agency); and by the National Institute of Allergy and Infectious Diseases Public Health Service research grants. S.K. was supported by JSPS Research Fellowships for Young Scientists.

REFERENCES

1. **Bauer, A., S. Chauvet, O. Huber, F. Usseglio, U. Rothbächer, D. Aragnol, R. Kemler, and J. Pradel.** 2000. Pontin52 and reptin52 function as antagonistic regulators of beta-catenin signalling activity. EMBO J. **19**:6121–6130.
2. **Cho, S. G., A. Bhoumik, L. Broday, V. Ivanov, B. Rosenstein, and Z. Ronai.** 2001. TIP49b, a regulator of activating transcription factor 2 response to stress and DNA damage. Mol. Cell. Biol. **21**:8398–8413.
3. **Elton, D., E. Medcalf, K. Bishop, and P. Digard.** 1999. Oligomerization of the influenza virus nucleoprotein: identification of positive and negative sequence elements. Virology **260**:190–200.
4. **Gallant, P.** 2007. Control of transcription by Pontin and Reptin. Trends Cell Biol. **17**:187–192.
5. **Gribun, A., K. L. Cheung, J. Huen, J. Ortega, and W. A. Houry.** 2008. Yeast Rvb1 and Rvb2 are ATP-dependent DNA helicases that form a heterohexameric complex. J. Mol. Biol. **376**:1320–1333.
6. **Hao, L., A. Sakurai, T. Watanabe, E. Sorensen, C. A. Nidom, M. A. Newton,**

P. Ahlquist, and Y. Kawaoka. 2008. *Drosophila* RNAi screen identifies host genes important for influenza virus replication. Nature **454**:890–893.
7. **Hatta, M., P. Gao, P. Halfmann, and Y. Kawaoka.** 2001. Molecular basis for high virulence of Hong Kong H5N1 influenza A viruses. Science **293**:1840–1842.
8. **Hu, C. D., and T. K. Kerppola.** 2003. Simultaneous visualization of multiple protein interactions in living cells using multicolor fluorescence complementation analysis. Nat. Biotechnol. **21**:539–545.
9. **Ikura, T., V. V. Ogryzko, M. Grigoriev, R. Groisman, J. Wang, M. Horikoshi, R. Scully, J. Qin, and Y. Nakatani.** 2000. Involvement of the TIP60 histone acetylase complex in DNA repair and apoptosis. Cell **102**:463–473.
10. **Kanemaki, M., Y. Kurokawa, T. Matsu-ura, Y. Makino, A. Masani, K. Okazaki, T. Morishita, and T. A. Tamura.** 1999. TIP49b, a new RuvB-like DNA helicase, is included in a complex together with another RuvB-like DNA helicase, TIP49a. J. Biol. Chem. **274**:22437–22444.
11. **Kerppola, T. K.** 2006. Complementary methods for studies of protein interactions in living cells. Nat. Methods **3**:969–971.
12. **King, T. H., W. A. Decatur, E. Bertrand, E. S. Maxwell, and M. J. Fournier.** 2001. A well-connected and conserved nucleoplasmic helicase is required for production of box C/D and H/ACA snoRNAs and localization of snoRNP proteins. Mol. Cell. Biol. **21**:7731–7746.
13. **Mayer, D., K. Molawi, L. Martínez-Sobrido, A. Ghanem, S. Thomas, S. Baginsky, J. Grossmann, A. García-Sastre, and M. Schwemmle.** 2007. Identification of cellular interaction partners of the influenza virus ribonucleoprotein complex and polymerase complex using proteomic-based approaches. J. Proteome Res. **6**:672–682.
14. **Nagata, K., A. Kawaguchi, and T. Naito.** 2008. Host factors for replication and transcription of the influenza virus genome. Rev. Med. Virol. **18**:247–260.
15. **Neumann, G., T. Watanabe, H. Ito, S. Watanabe, H. Goto, P. Gao, M. Hughes, D. R. Perez, R. Donis, E. Hoffmann, G. Hobom, and Y. Kawaoka.** 1999. Generation of influenza A viruses entirely from cloned cDNAs. Proc. Natl. Acad. Sci. USA **96**:9345–9350.
16. **Palese, P.** 2007. *Orthomyxoviridae*, p. 1647–1689. *In* D. M. Knipe, P. M. Howley, D. E. Griffin, R. A. Lamb, M. A. Martin, B. Roizman, and S. E. Straus (ed.), Fields virology, 5th ed. Lippincott Williams & Wilkins, Philadelphia, PA.
17. **Puri, T., P. Wendler, B. Sigala, H. Saibil, and I. R. Tsaneva.** 2007. Dodecameric structure and ATPase activity of the human TIP48/TIP49 complex. J. Mol. Biol. **366**:179–192.
18. **Shen, X., G. Mizuguchi, A. Hamiche, and C. Wu.** 2000. A chromatin remodelling complex involved in transcription and DNA processing. Nature **406**:541–544.
19. **Shinya, K., S. Hamm, M. Hatta, H. Ito, T. Ito, and Y. Kawaoka.** 2004. PB2 amino acid at position 627 affects replicative efficiency, but not cell tropism, of Hong Kong H5N1 influenza A viruses in mice. Virology **320**:258–266.
20. **Watkins, N. J., I. Lemm, D. Ingelfinger, C. Schneider, M. Hossbach, H. Urlaub, and R. Lührmann.** 2004. Assembly and maturation of the U3 snoRNP in the nucleoplasm in a large dynamic multiprotein complex. Mol. Cell **16**:789–798.
21. **Wood, M. A., S. B. McMahon, and M. D. Cole.** 2000. An ATPase/helicase complex is an essential cofactor for oncogenic transformation by c-Myc. Mol. Cell **5**:321–330.
22. **Ye, Q., R. M. Krug, and Y. J. Tao.** 2006. The mechanism by which influenza A virus nucleoprotein forms oligomers and binds RNA. Nature **444**:1078–1082.

JOURNAL OF VIROLOGY, May 2010, p. 5140–5147 Vol. 84, No. 10
0022-538X/10/$12.00 doi:10.1128/JVI.02021-09

Different Potential of C-Type Lectin-Mediated Entry between Marburg Virus Strains[▽]

Keita Matsuno,[1] Noriko Kishida,[2] Katsuaki Usami,[3] Manabu Igarashi,[1] Reiko Yoshida,[1] Eri Nakayama,[1] Masayuki Shimojima,[4] Heinz Feldmann,[5]† Tatsuro Irimura,[3] Yoshihiro Kawaoka,[4] and Ayato Takada[1]*

Department of Global Epidemiology, Hokkaido University Research Center for Zoonosis Control, Sapporo, Japan[1]; Laboratory of Influenza Virus Surveillance, Center for Influenza Virus Research, National Institute of Infectious Diseases, Tokyo, Japan[2]; Graduate School of Pharmaceutical Science, University of Tokyo, Tokyo, Japan[3]; Division of Virology, Department of Microbiology and Immunology, Institute of Medical Science, University of Tokyo, Tokyo, Japan[4]; and Special Pathogens Program, National Microbiology Laboratory, Public Health Agency of Canada, Winnipeg, Manitoba, Canada[5]

Received 24 September 2009/Accepted 25 February 2010

The glycoproteins (GPs) of filoviruses are responsible for virus entry into cells. It is known that GP interacts with cellular C-type lectins for virus attachment to cells. Since primary target cells of filoviruses express C-type lectins, C-type lectin-mediated entry is thought to be a possible determinant of virus tropism and pathogenesis. We compared the efficiency of C-type lectin-mediated entry between Marburg virus strains Angola and Musoke by using a vesicular stomatitis virus (VSV) pseudotype system. VSV pseudotyped with Angola GP (VSV-Angola) infected K562 cells expressing the C-type lectin, human macrophage galactose-type C-type lectin (hMGL), or dendritic cell-specific ICAM-3-grabbing nonintegrin (DC-SIGN) more efficiently than VSV pseudotyped with Musoke GP (VSV-Musoke). Unexpectedly, the binding affinity of the C-type lectins to the carbohydrates on GPs did not correlate with the different efficiency of C-type lectin-mediated entry. Site-directed mutagenesis identified the amino acid at position 547, which switched the efficiency of C-type lectin-mediated entry. In a three-dimensional model of GP, this amino acid was in close proximity to the putative site of cathepsin processing. Interestingly, the cathepsin inhibitors reduced the infectivity of VSV-Angola less efficiently than that of VSV-Musoke in C-type lectin-expressing K562 cells, whereas only a limited difference was found in control cells. The amino acid at position 547 was critical for the different effects of the inhibitors on the virus infectivities. These results suggest that the efficiency of C-type lectin-mediated entry of filoviruses is controlled not only by binding affinity between C-type lectins and GP but also by mechanisms underlying endosomal entry, such as proteolytic processing by the cathepsins.

Marburg virus (MARV) and Ebola virus (EBOV), which belong to the family *Filoviridae*, have produced sporadic outbreaks of hemorrhagic fever in Africa. After the initial outbreak of MARV infection in 1967 in Europe, which resulted in 7 deaths among 32 confirmed patients (41), there were three small, isolated outbreaks of MARV infection in Africa between 1975 and 1987. During one of the outbreaks in Kenya in 1980, one of the two patients died (42), and experimental studies showed that this Kenyan MARV Musoke strain (Musoke) killed monkeys within 12 days after infection (6). On the other hand, throughout a recent outbreak of MARV infection in Angola, 84% of the 422 patients died (29). This MARV Angola strain (Angola) produced fatal disease in monkeys within 8 days after inoculation and was thought to be more pathogenic than the Musoke strain (5, 17). Among EBOVs, a difference in pathogenicity was also suggested. Zaire EBOV is thought to be the most pathogenic EBOV, killing approximately up to 90% of patients, whereas Reston EBOV has never caused lethal infection in humans (31) and is less pathogenic in experimentally infected nonhuman primates than Zaire EBOV (16). However, the factors that influence the different pathogenicity among filoviruses remain unclear.

The envelope glycoprotein (GP) of filoviruses is the only spike protein and is responsible for both receptor binding and membrane fusion. GP is comprised of two molecules, GP1 and GP2, which are linked by a disulfide bond. GP1 contains the receptor-binding domain, which is responsible for the viral attachment to cell surface molecules (9, 25). GP2 has the heptad repeat regions required for assembling GP as a trimer and the internal fusion loop, which is thought to interact with the cellular membrane (50). Although the trigger to promote the conformational change leading to membrane fusion is not fully understood, it was recently suggested that endosomal proteolysis of EBOV GP by cysteine proteases such as cathepsins B and L plays an important role in inducing membrane fusion (4).

Both MARV and EBOV GPs are heavily glycosylated and contain both N- and O-linked carbohydrate chains with different terminal sialylation patterns that seem to depend on the virus strains and cell lines used for virus propagation (12, 18,

* Corresponding author. Mailing address: Department of Global Epidemiology, Hokkaido University Research Center for Zoonosis Control, Kita-20, Nishi-10, Kita-ku, Sapporo 001-0020, Japan. Phone: 81-11-706-9502. Fax: 81-11-706-7310. E-mail: atakada@czc.hokudai.ac.jp.

† Present address: Laboratory of Virology, Rocky Mountain Laboratories, Division of Intramural Research, National Institute of Allergy and Infectious Diseases, National Institutes of Health, Hamilton, MT 59840.

▽ Published ahead of print on 10 March 2010.

39, 48). The middle one-third of the GP molecule particularly varies among filoviruses and includes a mucin-like region (MLR) that contains a number of potential N- and O-linked glycosylation sites (32, 52). It is thought that carbohydrate chains on GP are recognized by cellular C-type lectins, such as the liver-specific C-type lectin asialoglycoprotein receptor (ASGP-R) (3), dendritic cell-specific ICAM-3-grabbing nonintegrin (DC-SIGN), liver/lymph node-SIGN (L-SIGN) (1, 2, 20, 30, 33, 40), human macrophage galactose-type C-type lectin (hMGL) (46), and liver and lymph node sinusoidal endothelial cell C-type lectin (LSECtin) (8, 19, 20, 34). While these C-type lectins show different specificities, depending on the structures of target glycans, all have been reported to promote filovirus entry. Hepatocytes, dendritic cells (DCs), monocytes, and macrophages are thought to be the preferred target cells of filoviruses, and infection of these cells is important for hemorrhagic manifestation and immune disorders (7, 13, 15, 36). Thus, increased infection of these cells might be directly involved in the pathogenesis of filoviruses (16).

In the present study, using the vesicular stomatitis virus (VSV) pseudotype system (VSV that contains the green fluorescent protein [GFP] gene rather than the receptor-binding GP gene [VSVΔG*]) described previously (45), we compared the properties of Angola and Musoke GPs and found a significant difference in the ability to utilize hMGL and DC-SIGN for their entry. Importantly, GP binding affinity for the C-type lectins was not the primary factor contributing to the difference. We identified a single amino acid involved in the different efficiency of C-type lectin-mediated entry between Angola and Musoke. Three-dimensional analysis suggested that this amino acid might affect the processing of GP by endosomal cysteine proteases and/or flexibility of the GP internal fusion loop. Here, mechanisms underlying the different efficiencies for C-type lectin-mediated entry of filoviruses are discussed.

MATERIALS AND METHODS

Viruses and cells. VSVΔG* expressing GFP pseudotyped with MARV GPs was generated as previously described (45). The viruses were treated with neutralizing monoclonal antibody I1 to VSV G protein before use (28). The virus titer was determined by counting the number of cells expressing GFP using fluorescence microscopy or flow cytometry.

Vero E6 and HEK293T cells were grown in Dulbecco's modified Eagle's medium supplemented with 10% fetal bovine serum, L-glutamine, and antibiotics. Human chronic myelogenous leukemia (K562) cells were grown in RPMI 1640 supplemented with 10% fetal bovine serum, L-glutamine, and antibiotics. K562 clones expressing hMGL (K562/hMGL) were generated as previously described (46). cDNA encoding DC-SIGN was isolated from a placenta cDNA library (Invitrogen) and then cloned into a mammalian cell expression vector, pcDNA3.1(+) (Invitrogen). K562 cells were transfected with the plasmid using Attractene transfection reagent (Qiagen). After selection with Geneticin (G418 sulfate; Calbiochem), DC-SIGN-positive cells (K562/DC-SIGN) were enriched with immunomagnetic beads by using monoclonal antibody CD209 (Beckman Coulter). K562 cells transfected with the empty vector pcDNA3.1(+) and selected by Geneticin were used as control cells (K562/mock).

Expression of soluble recombinant hMGL and DC-SIGN. Soluble hMGL was purified by affinity chromatography on a column of galactose-Sepharose 4B as described previously (44). The expression plasmid pET-15b encoding the extracellular domain (ECD) of DC-SIGN was similarly constructed. The plasmid was subsequently used to transform *Escherichia coli* BL21/DE3 pLysS. The recombinant DC-SIGN ECD was prepared from inclusion bodies in *E. coli*. The recombinant DC-SIGN ECD was bound to mannose-Sepharose 4B and eluted with 10 mM EDTA. Subsequently, biotinylation of these soluble proteins was performed using EZ-Link sulfo-NHS-LC-biotin (Pierce).

Lectin-ELISA analysis. VSVΔG* pseudotyped with GPs was purified by ultracentrifugation through a 25% sucrose cushion and diluted to give a titer of 5×10^5 infectious units (IU)/ml in phosphate-buffered saline (PBS). Enzyme-linked immunosorbent assay (ELISA) plates were coated with the viruses and then blocked with 3% bovine serum albumin in PBS. After each well was washed with Dulbecco's Tris-buffered saline (dTBS), biotinylated hMGL or DC-SIGN in dTBS was added. To detect C-type lectins bound to the viruses, horseradish peroxidase (HRP)-streptavidin (Jackson ImmunoResearch) and 3,3′,5,5′-tetramethylbenzidine (Sigma) were used.

Mutagenesis. To construct the mutant GPs, MARV GP cDNAs were cloned into the pATX vector, kindly provided by H. Ebihara (Laboratory of Virology, Department of Health and Human Services, Rocky Mountain Laboratories, Division of Intramural Research, NIAID, NIH). By using the primers containing the sequences of the desired regions and the class IIS restriction enzyme, the BsmBI site, the MLR-deletion mutant, and chimeric GP constructs were generated. Mutant GPs with a single substitution (A/H504T, A/G547V, A/A596T, A/R618K, M/T504H, M/V547G, M/T596A, and M/K618R) were generated by using the primers containing the desired mutations and the BsmBI site. All the mutant GP genes were cloned into pCAGGS, the mammalian expression plasmid, and used for expression of the GPs in HEK293T cells.

Virus titration. The infectivity of VSVΔG* pseudotyped with GPs on K562 clones was determined by counting the number of GFP-positive cells using flow cytometry. To test C-type lectin-mediated entry, 10^5 cells of the K562 clones in 96-well plates were infected with the respective viruses, whose titers were standardized (i.e., all the viruses were diluted to give 1×10^5 to 5×10^5 IU/ml in Vero E6 cells that uniformly gave approximately 1×10^4 to 5×10^4 IU/ml in K562/mock cells), and the number of GFP-positive cells were counted. To investigate the effects of the cathepsin B and L inhibitors, CA-074Me and FY-dmk, respectively (Calbiochem), cells were treated with one of the inhibitors for 3 h before infection.

Binding assay. Approximately 10^6 infectious units (in Vero E6 cells) of purified VSVΔG* pseudotyped with GPs were incubated with 10^5 cells of K562/hMGL and K562/DC-SIGN for 1 h on ice. After being washed three times with PBS(+), cells were lysed to measure the amount of VSV matrix protein in the virions which bound on the cell surface.

SDS-PAGE and Western blotting. Cells or purified viruses were lysed with PBS containing 1% Triton X-100 and protease inhibitor cocktail Complete Mini (Roche), and the insoluble fraction was removed by centrifugation. Lysates were mixed with Laemmli sample buffer (Bio-Rad), electrophoresed by sodium dodecyl sulfate-polyacrylamide gel electrophoresis (SDS-PAGE) on 10 to 20% SuperSep (Wako), and blotted on a polyvinylidene difluoride (PVDF) membrane (Millipore). Non-specific binding to the membrane was blocked with 3% skim milk in PBS. A mixture of the sera obtained from mice immunized with Angola virus-like particles and Musoke virus-like particles for detecting MARV GPs or anti-VSV matrix protein monoclonal antibody (195-2) was incubated with the membrane. Peroxidase-conjugated AffiniPure goat anti-mouse IgG(H+L) (Jackson ImmunoResearch) and Immobilon Western (Millipore) were used for visualization. Intensities of specific bands were measured with ATTO CS Analyzer 2.1.

Molecular modeling. A three-dimensional model of Angola GP was generated by a homology modeling method using the crystal structure of EBOV GP (Protein Data Bank [PDB] code 3CSY) (27) as a template. The sequence alignment between MARV and EBOV GPs was based on that previously reported by Lee et al. (27). One hundred models of the first construction were generated using the automodel class in Modeller 9v6 (35), and the model with the lowest value of the Modeller objective function was selected. Next, to fill the gap of some potential loop conformation that the structural template of Zaire EBOV GP lacks (residues 174 to 197, 208 to 218, and 272 to 291 in the Angola GP numbering that correspond to residues 190 to 213, 224 to 225, and 279 to 298 in Zaire EBOV GP, respectively), two hundred models were generated by the loop model class (14). The best loop model was chosen by a combination of the Modeller objective function value and the discrete optimized protein energy (DOPE) statistical potential score (38). Then, the model, after addition of hydrogen atoms, was refined by energy minimization (EM) with the minimization protocols in the Discovery Studio 2.1 software package (Accelrys, San Diego, CA), using a CHARMM force field. Steepest descent, followed by conjugate gradient minimizations, was carried out until the root mean square (RMS) gradient was less than or equal to 0.01 kcal/mol/Å. The generalized Born implicit solvent model (43, 47) was used to model the effects of solvation. The model of Angola GP was finally evaluated by using PROCHECK (26), WHAT_CHECK (22), and Verify3D (10).

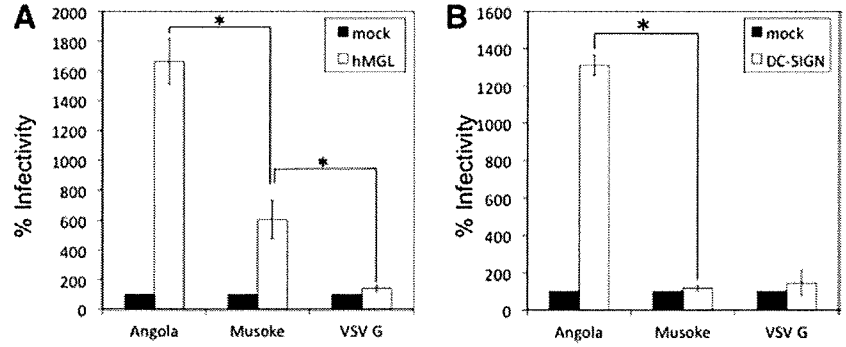

FIG. 1. Infectivity of VSVΔG* pseudotyped with MARV GPs in K562 cells expressing the C-type lectins. The infectivities of VSV-Angola and -Musoke were standardized using Vero E6 cells, as described in Materials and Methods, and approximately the same titers of viruses were used to infect K562/mock, K562/hMGL, and K562/DC-SIGN cells. The infected cells were counted using a flow cytometer, and the percentages of infectivity (i.e., relative infectivities) in K562/hMGL (A) and K562/DC-SIGN (B) cells were determined by setting the number of the infected K562/mock cells to 100% (46). All experiments were done in triplicate, and average results and standard deviations are shown. Statistical significance was determined by Student's *t* test. *, $P < 0.05$.

RESULTS

Efficiency of C-type lectin-mediated entry differs between MARV strains. We generated VSVΔG* bearing VSV G (VSV-VSV G), VSVΔG* bearing Angola GP (VSV-Angola), or VSVΔG* bearing Musoke GP (VSV-Musoke), and the infectivities of these viruses in K562/hMGL or K562/DC-SIGN cells were compared (Fig. 1). No significant enhancement of VSV-VSV G infectivity was seen in these C-type lectin-expressing cells. Consistent with a previous study (46), the viruses infected K562/hMGL cells more efficiently than they infected control K562/mock cells. In K562/DC-SIGN cells, the difference was observed only for VSV-Angola infectivity. It was noted that VSV-Angola showed significantly higher infectivity in these C-type lectin-expressing cells than VSV-Musoke, as was seen between Zaire and Reston EBOVs (46).

hMGL and DC-SIGN bind to MARV GPs in a different manner. To test the attachment of VSV-Angola and -Musoke to the surfaces of the cells expressing C-type lectins, a direct binding assay was performed (Fig. 2A). In both K562/hMGL and K562/DC-SIGN cells, only limited differences of the viruses attached on the cell surfaces were observed. For more quantitative analysis of the binding of MARV GPs to the C-type lectins, we next carried out a lectin-ELISA using soluble forms of hMGL and DC-SIGN and purified viruses (Fig. 2B and C). We found that both lectins bound to Angola and Musoke GPs in a dose-dependent manner and that hMGL had slightly higher ability to bind to Angola GPs than to bind to Musoke GPs, whereas DC-SIGN similarly bound to both GPs, confirming the different glycan specificities of these lectins (i.e., hMGL and DC-SIGN preferentially react with O-glycans and high-mannose-type N-glycans, respectively) (11, 21, 44).

MLRs and GP2 are important for efficient entry mediated by C-type lectins. MLRs of filoviruses have been shown to play an important role in interaction with the C-type lectins. To ascertain the contribution of the MLR of MARV GP to C-type lectin-mediated entry, we first constructed MLR-deletion mutants (AΔ and MΔ) (Fig. 3A) and examined the infectivities of VSVΔG* pseudotyped with these mutant GPs (VSV-AΔ and -MΔ) in Vero E6, K562/hMGL, and K562/DC-SIGN cells. VSV-AΔ and -MΔ showed no defects in their infectivities in Vero E6 cells, consistent with a previous study (32), indicating that glycosylation in the MLR and GP cleavage by furin are not essential to infect Vero E6 cells. In contrast, these viruses infected K562 cells expressing the C-type lectins much less efficiently than VSVΔG* pseudotyped with full-length wild-type GPs (Fig. 3B and C). These results indicate the major contribution of the MLR to C-type lectin-mediated entry of MARV.

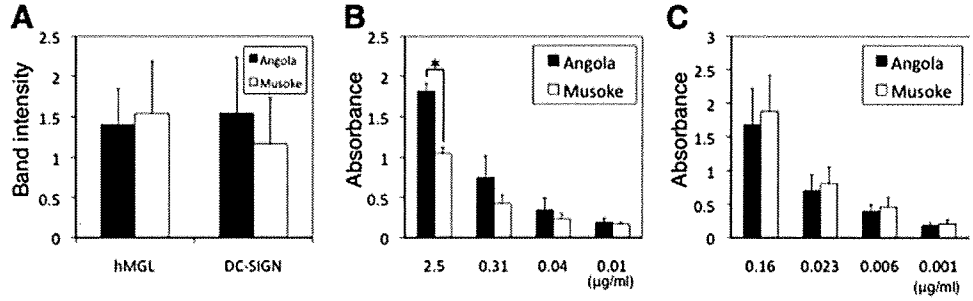

FIG. 2. Binding affinity of the C-type lectins to VSVΔG* pseudotyped with MARV GPs. (A) The amounts of VSV-Angola and -Musoke that attached on K562/hMGL or K562/DC-SIGN cells were shown as band intensities of VSV matrix protein. (B, C) A lectin-ELISA was performed, using purified VSV-Angola and -Musoke as antigens. Biotinylated recombinant soluble hMGL (B) and DC-SIGN ECD (C) were incubated at the indicated concentrations and visualized, as described in Materials and Methods. All experiments were done in triplicate, and average results and standard deviations are shown. Statistical significance was determined by Student's *t* test. *, $P < 0.05$.

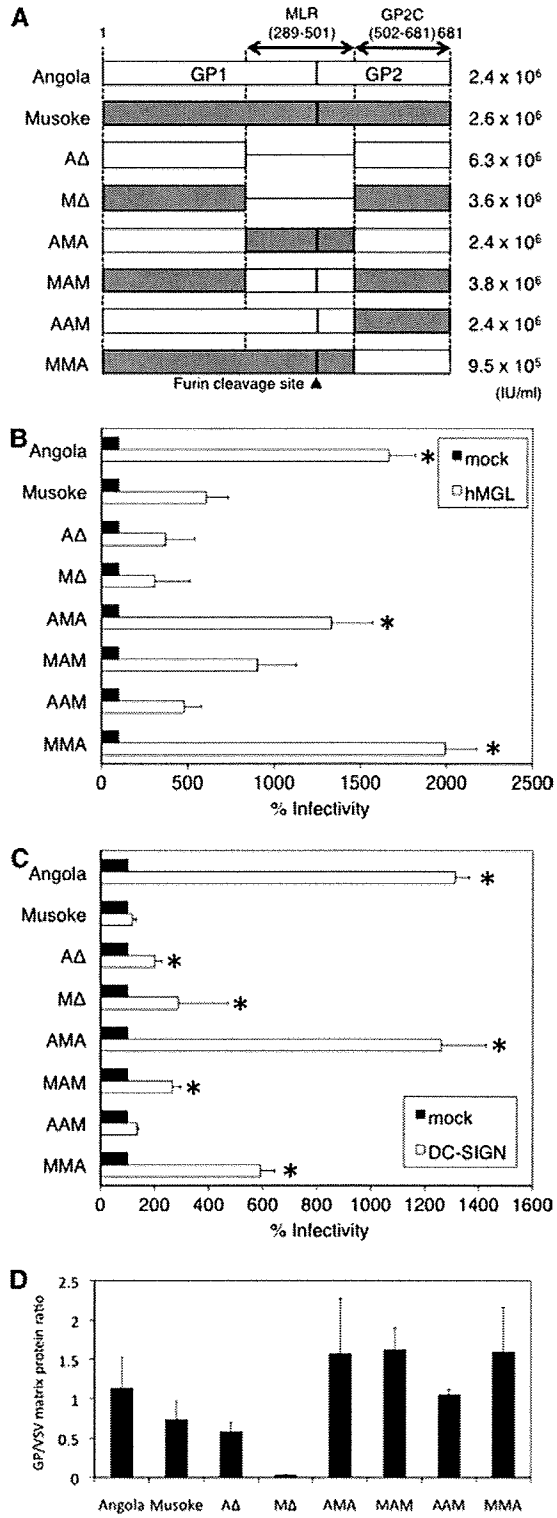

FIG. 3. Infectivity of VSVΔG* pseudotyped with the deletion or chimeric mutant GPs in C-type lectin-expressing cells. (A) The names of the MARV mutant GPs and the relevant amino acid positions are shown in the schematic. The number of infectious units determined for each virus in Vero E6 cells are shown on the right. (B, C) The relative infectivities of the viruses in K562/hMGL (B) and K562/DC-SIGN (C) cells were determined, as described in the legend of Fig. 1. All experiments were done in triplicate, and average results and standard deviations are shown. Statistical significance was determined (compared to the infectivity of VSV-Musoke in each K562/hMGL or K562/DC-SIGN cell) by Student's t test. *, $P < 0.05$. (D) The amounts of mutant GPs incorporated within the pseudotyped VSVΔG* were quantitated by using Western blotting of purified virions. Band intensities of MARV GPs and VSV matrix protein were determined, and their ratios are shown.

Next, we constructed chimeric GPs whose MLRs were swapped (AMA and MAM) (Fig. 3A), and the infectivities of VSVΔG* pseudotyped with these chimeric GPs (VSV-AMA and VSV-MAM) were tested (Fig. 3B and C). Unexpectedly, the relative infectivity of VSV-AMA in K562 cells expressing the C-type lectins was significantly higher than that of VSV-Musoke and similar to that of VSV-Angola. Replacement of the MLR of Musoke GP with that of Angola GP (MAM) showed only minimal effects on the enhancement of infectivity in the C-type lectin-expressing cells if compared with VSV-Musoke infectivity.

We finally replaced amino acid positions 502 to 681 of the GP2 regions (GP2C) of each (AAM and MMA) (Fig. 3A) and found that VSVΔG* pseudotyped with the chimeric Angola GP that had Musoke GP2C (VSV-AAM) infected both K562/hMGL and K562/DC-SIGN cells less efficiently than VSV-Angola (Fig. 3B and C), and the relative infectivities of VSV-AAM were similar to that of VSV-Musoke in both C-type lectin-expressing cell types. In contrast, the infectivities of VSV-MMA in both types of cells were significantly higher than that of VSV-Musoke or -AAM. These results indicate that GP2C is critical for the difference in the efficiency of C-type lectin-mediated entry between VSV-Angola and -Musoke. It was confirmed that all the chimeric GPs were similarly incorporated into virions (Fig. 3D). MΔ was not clearly detected by Western blotting. It was most likely due to the lack of the MLR containing many specific epitopes, resulting in the different reactivity of polyclonal serum to MΔ. We further confirmed that fully functional GPs were incorporated into VSV virions, since there is no significant difference in the infectivities in Vero E6 cells among these viruses.

Substitution of an amino acid at position 547 in the GP2 region influences the efficiency of C-type lectin-mediated entry. There are four different amino acids in GP2C between the Angola and Musoke GPs. To identify which amino acid(s) contributes to the different ability of C-type lectin-mediated entry between the Angola and Musoke strains, the following eight mutant GPs that contain single-amino-acid substitutions were constructed: four Angola-based mutant GPs (A/H504T, A/G547V, A/A596T, and A/R618K) and four Musoke-based mutant GPs (M/T504H, M/V547G, M/T596A, and M/K618R) (Fig. 4A). The infectivity levels of VSVΔG* pseudotyped with these mutant GPs in K562/hMGL or K562/DC-SIGN cells were compared (Fig. 4B and C). While the mutations at position 504, 596, or 618 did not affect the infectivity of the respective viruses in cells expressing the C-type lectins, the infectivities of VSVΔG* pseudotyped with mutant GPs with substitution at position 547 (VSV-A/G547V and -M/V547G) were clearly switched (i.e., the relative infectivities of VSV-Angola and -M/V547A in the C-type lectin-expressing cells were comparable and higher than those of VSV-Musoke and -A/G547V).

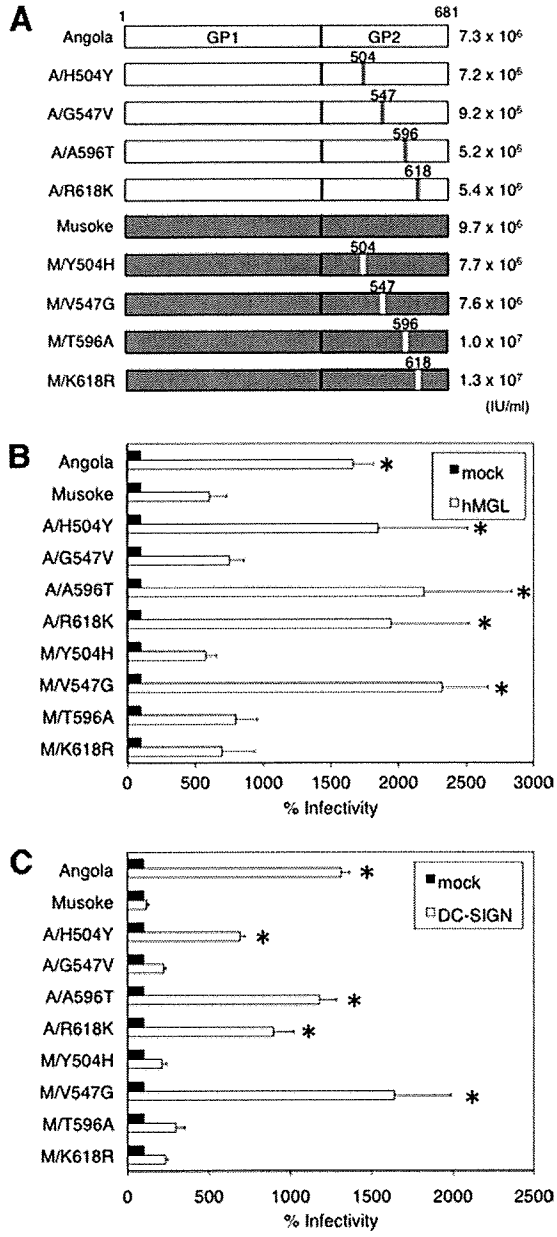

FIG. 4. Infectivity of VSVΔG* pseudotyped with the single-amino-acid mutant GPs in the C-type lectin-expressing cells. (A) The names of the MARV GP mutants and the positions of substituted amino acids are shown in the schematic. The number of infectious units determined for each virus in Vero E6 cells are shown on the right. (B, C) The relative infectivities of the viruses in K562/hMGL (B) and K562/DC-SIGN (C) cells were determined, as described in the legend of Fig. 1. All experiments were done in triplicate, and average results and standard deviations are shown. Statistical significance was determined (compared to the infectivity of VSV-Musoke in each K562/hMGL or K562/DC-SIGN cell) by Student's *t* test. *, $P < 0.05$.

Infectivities of VSV-Angola and -Musoke are reduced in different manners by cathepsin inhibitors in the C-type lectin-expressing cells. Because the GP binding affinity for C-type lectins (i.e., attachment) did not seem essential for the different ability levels of C-type lectin-mediated entry between the Angola and Musoke strains, we then focused on the following

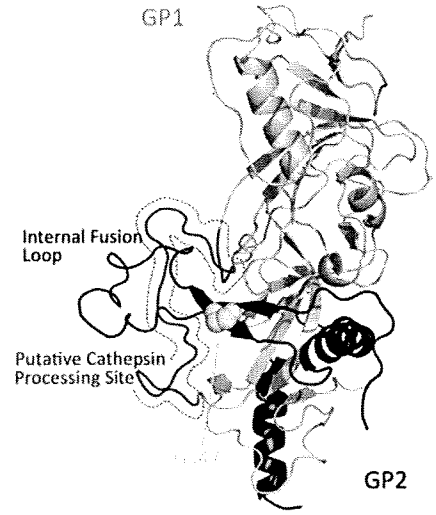

FIG. 5. Three-dimensional structure of the Angola GP monomer. The crystal structure of EBOV GP (PDB code 3CSY) was used as a template for homology modeling. GP1 (lime green) and GP2 (dark blue) are shown as ribbon models. Glycine at position 547 (G547, yellow) is shown as a space-filling model. The putative cathepsin cleavage site (amino acid residues 174 to 197 of Angola GP, corresponding to amino acid residues 190 to 213 of Zaire EBOV GP) is colored in red. This figure was prepared using PyMOL (DeLano Scientific LLC).

steps of viral entry. In EBOV and human coronavirus entry, it has been reported that proteolysis of GP by cellular endosomal cysteine proteases cathepsins B and/or L is necessary (4, 23, 24, 37). A three-dimensional model of Angola GP revealed that glycine at position 547 of Angola GP is presumed to form a β strand included in the internal fusion loop and is in close proximity to the putative cathepsin processing site (Fig. 5) (9, 27). Thus, we hypothesized that the amino acid change at position 547 affected the efficiency of cathepsin processing, which might lead to membrane fusion.

To test our hypothesis, VSVΔG* pseudotyped with wild-type or mutant (A/G547V and M/V547G) GPs was analyzed by comparing the infectivities of these viruses in Vero E6, control K562/mock, K562/hMGL, and K562/DC-SIGN cells pretreated with cathepsin inhibitors (Fig. 6). The infectivities of all the viruses were reduced by both of the inhibitors in a dose-dependent manner in all cells tested, suggesting that the proteolysis of GP by cathepsins B and/or L is also required for MARV entry. Interestingly, the infectivities of VSV-Angola and -M/V547G in K562 cells expressing the C-type lectins were less effectively reduced by these cathepsin inhibitors than those of VSV-Musoke and -A/G547V, whereas in Vero E6 and K562/mock cells, the differences in the infectivity at each concentration of the inhibitors were limited among the viruses. Paired Student's *t* test revealed significant differences ($P < 0.01$) in the following pairs: VSV-Angola and -Musoke, VSV-Angola and -A/G547C, and VSV-Musoke and -M/V547G (Fig. 6C, G, and H). And in Fig. 6D, the significant differences among these viruses were observed at a concentration of 10 μM by Student's *t* test. The infectivities of VSVΔG* pseudotyped with the other mutant GPs (i.e., VSV-A/H504T, -A/A596T, -A/

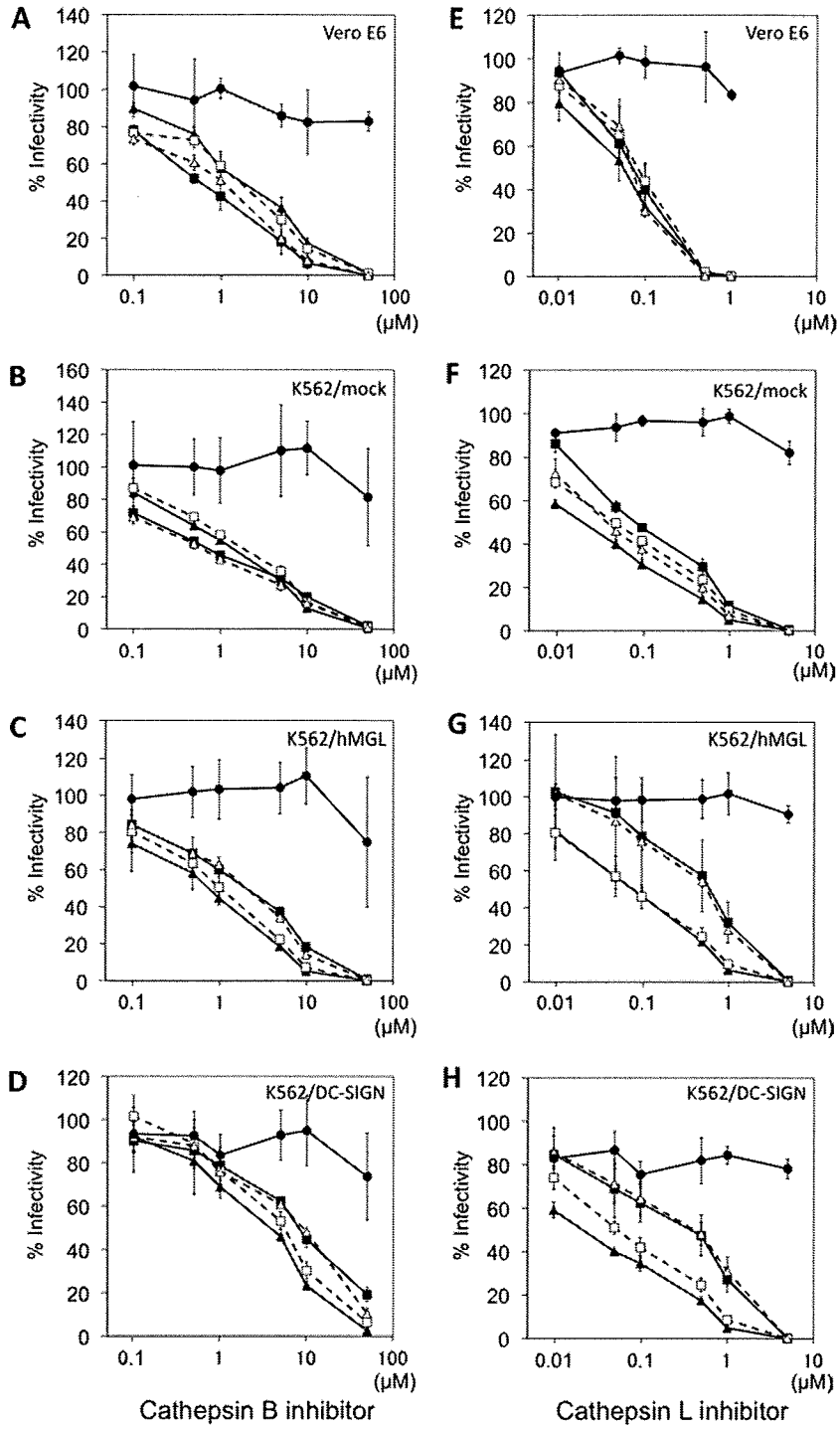

FIG. 6. Inhibition of virus infectivity by cathepsin inhibitors. Vero E6 (A and E), K562/mock (B and F), K562/hMGL (C and G), and K562/DC-SIGN (D and H) cells were pretreated with cathepsin B inhibitor (A, B, C, and D), cathepsin L inhibitor (E, F, G, and H), or dimethyl sulfoxide (DMSO) for 3 h and then infected with VSV-Angola (closed square), -Musoke (closed triangle), -A/G547V (open square), -M/V547G (open triangle) or -VSV G (closed circle). The number of infected cells, given in DMSO-treated cells, was used to set the 100% infectivity level for each cell type, and the relative infectivity was determined at each concentration of the inhibitors. All experiments were done in triplicate, and average results and standard deviations are shown.

R618K, -M/T504H, -M/T596A, and -M/K618R) were reduced by these cathepsin inhibitors similar to those of VSVΔG* pseudotyped with the respective wild-type GPs (data not shown).

DISCUSSION

It has been shown that cellular C-type lectins are utilized for the attachment of several viruses to host cells. hMGL, which

was originally founded as a macrophage-specific C-type lectin recognizing galactose/*N*-acetylgalactosamine, is expressed in monocyte-derived DCs and macrophages (44), and it was demonstrated that hMGL promoted the infection of EBOV and MARV (46). DC-SIGN, which recognizes high-mannose-type N-glycans and plays an important role in regulating the immune system (53), has also been shown to promote infection by several viruses (e.g., Ebola, Marburg, human immunodeficiency, hepatitis C, measles, dengue, and influenza viruses) (49, 53). A liver-specific C-type lectin, ASGP-R, which recognizes galactose in carbohydrate side chains, has been shown to be exploited for MARV infection of hepatocytes (3) and is thought to be one of the possible determinants of hepatotropism of MARV (17). Taken together, increased infection of these cells expressing C-type lectins and subsequent destruction of the host immune functions and coagulation system may be crucial for the pathogenesis of filoviruses. Our previous study (46) and the present study show that the different abilities used to utilize the C-type lectins among filoviruses to promote cellular entry might be correlated with the pathogenicities of the viruses. *In vivo* study may be needed to provide a direct link between the pathogenicity of MARV and its ability to use C-type lectins for entry into target cells.

Using deletion mutant GPs, we found that both hMGL and DC-SIGN principally recognized MLRs. Amino acid comparison between Angola and Musoke GPs indicates that the similarity of their MLRs is 86.4% (data not shown). The numbers of potential O-glycosylation sites vary between Angola and Musoke GPs (the number of these sites for Musoke GP is less than the number of these sites for Angola GP), whereas the potential N-glycosylation sites are relatively conserved, supporting our observation that hMGL, but not DC-SIGN, bound more efficiently to Angola GP than to Musoke GP in the lectin-ELISA. However, using chimeric mutant GPs, we showed that the structure of the MLR itself was not essential for the different levels of infectivity between VSV-Angola and -Musoke in K562 cells expressing these C-type lectins, suggesting that the capacity of the GP for binding to C-type lectins through the MLR (i.e., the glycosylation pattern of MLR) is not the only factor contributing to the efficiency of C-type lectin-mediated entry. Indeed, we identified that the amino acid at position 547 in GP2, but not in the MLR, was critical for the different efficiency levels of C-type lectin-mediated entry between VSV-Angola and -Musoke. It is of interest to confirm the importance of this amino acid in MARV infection by using a reverse genetics approach.

In our three-dimensional model, it seemed unlikely that glycine/valine at position 547 directly influenced the binding to the putative specific receptors, since substitution of this amino acid did not affect the infectivity of pseudotyped viruses in Vero E6 or control K562 cells (data not shown), and this amino acid was not located around the putative receptor-binding domain (9, 25). We showed that the effects of cathepsin inhibitors on the infectivity differ between Angola and Musoke only in the C-type lectin-expressing cells, and the single-amino-acid substitution at position 547 altered the effects of cathepsin inhibitors. However, no significant difference in the susceptibility to cathepsins was seen in direct digestion assays *in vitro* using soluble forms of the C-type lectins and purified virions (data not shown). These results suggest that glycine at position 547 increases sensitivity of GPs to endosomal cathepsins during C-type lectin-mediated entry, but our *in vitro* digestion assay did not provide actual conditions for interaction between GPs and C-type lectins in endosomes. It may be also possible that when the viruses are internalized to endosomes through the interaction with C-type lectins, (i) the amino acid at position 547 affects the flexibility of the fusion loop and/or the efficiency of conformational change, and (ii) glycine at position 547 weakens GP1-GP2 interaction, resulting in reduced cathepsin dependence in virus entry, as reported with EBOV GP (51). It is interesting to clarify how this amino acid contributes to the intramolecule interaction required for GP functions.

In summary, our data suggest that the efficiency of C-type lectin-mediated entry of filoviruses is determined not only by direct interaction between GP and C-type lectins but also by some mechanisms underlying endosomal entry, such as proteolytic processing, and likely by cathepsins or membrane fusion machinery. Although further investigations are required to prove our hypotheses, this study provides new insights into understanding the molecular basis of the C-type lectin-mediated entry of filoviruses, which may have a possible link to their pathogenicity.

ACKNOWLEDGMENTS

We thank Hiroko Miyamoto, Ayaka Yokoyama, Teiji Murakami, and Aiko Ohnuma for technical assistance and Kim Barrymore for editing the manuscript.

This work was supported by Research Fellowships for Young Scientists from the Japan Society for the Promotion of Science, by Takeda Science Foundation, by a Grant-in-Aid for Scientific Research on Priority Areas (grant 19041001), and in part by the Program of Founding Research Centers for Emerging and Reemerging Infectious Diseases (grant 05021011) and the Global COE Program "Establishment of International Collaboration Centers for Zoonosis Control" (F-001) from the Ministry of Education, Culture, Sports, Science and Technology (MEXT), Japan (http://www.mext.go.jp/english/index.htm).

The funders had no role in study design, data collection and analysis, the decision to publish, or preparation of the manuscript.

REFERENCES

1. **Alvarez, C. P., F. Lasala, J. Carrillo, O. Muñiz, A. L. Corbí, and R. Delgado.** 2002. C-type lectins DC-SIGN and L-SIGN mediate cellular entry by Ebola virus in cis and in trans. J. Virol. **76**:6841–6844.
2. **Baribaud, F., S. Pöhlmann, G. Leslie, F. Mortari, and R. W. Doms.** 2002. Quantitative expression and virus transmission analysis of DC-SIGN on monocyte-derived dendritic cells. J. Virol. **76**:9135–9142.
3. **Becker, S., M. Spiess, and H. D. Klenk.** 1995. The asialoglycoprotein receptor is a potential liver-specific receptor for Marburg virus. J. Gen. Virol. **76**(Pt. 2):393–399.
4. **Chandran, K., N. J. Sullivan, U. Felbor, S. P. Whelan, and J. M. Cunningham.** 2005. Endosomal proteolysis of the Ebola virus glycoprotein is necessary for infection. Science **308**:1643–1645.
5. **Daddario-DiCaprio, K. M., T. W. Geisbert, J. B. Geisbert, U. Ströher, L. E. Hensley, A. Grolla, E. A. Fritz, F. Feldmann, H. Feldmann, and S. M. Jones.** 2006. Cross-protection against Marburg virus strains by using a live, attenuated recombinant vaccine. J. Virol. **80**:9659–9666.
6. **Daddario-DiCaprio, K. M., T. W. Geisbert, U. Ströher, J. B. Geisbert, A. Grolla, E. A. Fritz, L. Fernando, E. Kagan, P. B. Jahrling, L. E. Hensley, S. M. Jones, and H. Feldmann.** 2006. Postexposure protection against Marburg haemorrhagic fever with recombinant vesicular stomatitis virus vectors in nonhuman primates: an efficacy assessment. Lancet **367**:1399–1404.
7. **Davis, K. J., A. O. Anderson, T. W. Geisbert, K. E. Steele, J. B. Geisbert, P. Vogel, B. M. Connolly, J. W. Huggins, P. B. Jahrling, and N. K. Jaax.** 1997. Pathology of experimental Ebola virus infection in African green monkeys. Involvement of fibroblastic reticular cells. Arch. Pathol. Lab. Med. **121**:805–819.
8. **Dominguez-Soto, A., L. Aragoneses-Fenoll, E. Martin-Gayo, L. Martinez-Prats, M. Colmenares, M. Naranjo-Gomez, F. E. Borras, P. Munoz, M. Zubiaur, M. L. Toribio, R. Delgado, and A. L. Corbi.** 2007. The DC-SIGN-related lectin LSECtin mediates antigen capture and pathogen binding by human myeloid cells. Blood **109**:5337–5345.

9. **Dube, D., M. B. Brecher, S. E. Delos, S. C. Rose, E. W. Park, K. L. Schornberg, J. H. Kuhn, and J. M. White.** 2009. The primed ebolavirus glycoprotein (19-kilodalton $GP_{1,2}$): sequence and residues critical for host cell binding. J. Virol. **83**:2883–2891.
10. **Eisenberg, D., R. Lüthy, and J. U. Bowie.** 1997. VERIFY3D: assessment of protein models with three-dimensional profiles. Methods Enzymol. **277**:396–404.
11. **Feinberg, H., D. A. Mitchell, K. Drickamer, and W. I. Weis.** 2001. Structural basis for selective recognition of oligosaccharides by DC-SIGN and DC-SIGNR. Science **294**:2163–2166.
12. **Feldmann, H., S. T. Nichol, H. D. Klenk, C. J. Peters, and A. Sanchez.** 1994. Characterization of filoviruses based on differences in structure and antigenicity of the virion glycoprotein. Virology **199**:469–473.
13. **Feldmann, H., H. Bugany, F. Mahner, H. D. Klenk, D. Drenckhahn, and H. J. Schnittler.** 1996. Filovirus-induced endothelial leakage triggered by infected monocytes/macrophages. J. Virol. **70**:2208–2214.
14. **Fiser, A., R. K. G. Do, and A. Šali.** 2000. Modeling of loops in protein structures. Protein Sci. **9**:1753–1773.
15. **Geisbert, T. W., P. B. Jahrling, M. A. Hanes, and P. M. Zack.** 1992. Association of Ebola-related Reston virus particles and antigen with tissue lesions of monkeys imported to the United States. J. Comp. Pathol. **106**:137–152.
16. **Geisbert, T. W., and L. E. Hensley.** 2004. Ebola virus: new insights into disease aetiopathology and possible therapeutic interventions. Expert Rev. Mol. Med. **6**:1–24.
17. **Geisbert, T. W., K. M. Daddario-DiCaprio, J. B. Geisbert, H. A. Young, P. Formenty, E. A. Fritz, T. Larsen, and L. E. Hensley.** 2007. Marburg virus Angola infection of rhesus macaques: pathogenesis and treatment with recombinant nematode anticoagulant protein c2. J. Infect. Dis. **196**(Suppl. 2):S372–S381.
18. **Geyer, H., C. Will, H. Feldmann, H. D. Klenk, and R. Geyer.** 1992. Carbohydrate structure of Marburg virus glycoprotein. Glycobiology **2**:299–312.
19. **Gramberg, T., H. Hofmann, P. Möller, P. F. Lalor, A. Marzi, M. Geier, M. Krumbiegel, T. Winkler, F. Kirchhoff, D. H. Adams, S. Becker, J. Münch, and S. Pöhlmann.** 2005. LSECtin interacts with filovirus glycoproteins and the spike protein of SARS coronavirus. Virology **340**:224–236.
20. **Gramberg, T., E. Soilleux, T. Fisch, P. F. Lalor, H. Hofmann, S. Wheeldon, A. Cotterill, A. Wegele, T. Winkler, D. H. Adams, and S. Pöhlmann.** 2008. Interactions of LSECtin and DC-SIGN/DC-SIGNR with viral ligands: differential pH dependence, internalization and virion binding. Virology **373**: 189–201.
21. **Higashi, N., K. Fujioka, N. Denda-Nagai, S. Hashimoto, S. Nagai, T. Sato, Y. Fujita, A. Morikawa, M. Tsuiji, M. Miyata-Takeuchi, Y. Sano, N. Suzuki, K. Yamamoto, K. Matsushima, and T. Irimura.** 2002. The macrophage C-type lectin specific for galactose/N-acetylgalactosamine is an endocytic receptor expressed on monocyte-derived immature dendritic cells. J. Biol. Chem. **277**:20686–20693.
22. **Hooft, R. W. W., C. Sander, M. Scharf, and G. Vriend.** 1996. The PDBFINDER database: a summary of PDB, DSSP and HSSP information with added value. Comput. Appl. Biosci. **12**:525–529.
23. **Kaletsky, R. L., G. Simmons, and P. Bates.** 2007. Proteolysis of the Ebola virus glycoproteins enhances virus binding and infectivity. J. Virol. **81**:13378–13384.
24. **Kawase, M., K. Shirato, S. Matsuyama, and F. Taguchi.** 2009. Protease-mediated entry via the endosome of human coronavirus 229E. J. Virol. **83**:712–721.
25. **Kuhn, J. H., S. R. Radoshitzky, A. C. Guth, K. L. Warfield, W. Li, M. J. Vincent, J. S. Towner, S. T. Nichol, S. Bavari, H. Choe, M. J. Aman, and M. Farzan.** 2006. Conserved receptor-binding domains of Lake Victoria marburgvirus and Zaire ebolavirus bind a common receptor. J. Biol. Chem. **281**:15951–15958.
26. **Laskowski, R. A., M. W. MacArthur, D. S. Moss, and J. M. Thornton.** 1993. PROCHECK: a program to check the stereochemical quality of protein structures. J. Appl. Crystallogr. **26**:283–291.
27. **Lee, J. E., M. L. Fusco, A. J. Hessell, W. B. Oswald, D. R. Burton, and E. O. Saphire.** 2008. Structure of the Ebola virus glycoprotein bound to an antibody from a human survivor. Nature **454**:177–182.
28. **Lefrancois, L., and D. S. Lyles.** 1982. The interaction of antibody with the major surface glycoprotein of vesicular stomatitis virus. I. Analysis of neutralizing epitopes with monoclonal antibodies. Virology **121**:157–167.
29. **Ligon, B. L.** 2005. Outbreak of Marburg hemorrhagic fever in Angola: a review of the history of the disease and its biological aspects, p. 219–224. *In* C. R. Woods (ed.), Seminars in pediatric infectious diseases, vol. 16. Elsevier, New York, NY.
30. **Lin, G., G. Simmons, S. Pöhlmann, F. Baribaud, H. Ni, G. J. Leslie, B. S. Haggarty, P. Bates, D. Weissman, J. A. Hoxie, and R. W. Doms.** 2003. Differential N-linked glycosylation of human immunodeficiency virus and Ebola virus envelope glycoproteins modulates interactions with DC-SIGN and DC-SIGNR. J. Virol. **77**:1337–1346.
31. **Mahanty, S., and M. Bray.** 2004. Pathogenesis of filoviral haemorrhagic fevers. Lancet Infect. Dis. **4**:487–498.
32. **Manicassamy, B., J. Wang, E. Rumschlag, S. Tymen, V. Volchkova, V. Volchkov, and L. Rong.** 2007. Characterization of Marburg virus glycoprotein in viral entry. Virology **358**:79–88.
33. **Marzi, A., T. Gramberg, G. Simmons, P. Möller, A. J. Rennekamp, M. Krumbiegel, M. Geier, J. Eisemann, N. Turza, B. Saunier, A. Steinkasserer, S. Becker, P. Bates, H. Hofmann, and S. Pöhlmann.** 2004. DC-SIGN and DC-SIGNR interact with the glycoprotein of Marburg virus and the S protein of severe acute respiratory syndrome coronavirus. J. Virol. **78**:12090–12095.
34. **Powlesland, A. S., T. Fisch, M. E. Taylor, D. F. Smith, B. Tissot, A. Dell, S. Pöhlmann, and K. Drickamer.** 2008. A novel mechanism for LSECtin binding to Ebola virus surface glycoprotein through truncated glycans. J. Biol. Chem. **283**:593–602.
35. **Šali, A.** 1995. Comparative protein modeling by satisfaction of spatial restraints. Mol. Med. Today **234**:779–815.
36. **Schnittler, H. J., and H. Feldmann.** 1999. Molecular pathogenesis of filovirus infections: role of macrophages and endothelial cells. Curr. Top. Microbiol. Immunol. **235**:175–204.
37. **Schornberg, K., S. Matsuyama, K. Kabsch, S. Delos, A. Bouton, and J. White.** 2006. Role of endosomal cathepsins in entry mediated by the Ebola virus glycoprotein. J. Virol. **80**:4174–4178.
38. **Shen, M., and A. Šali.** 2006. Statistical potential for assessment and prediction of protein structures. Protein Sci. **15**:2507–2524.
39. **Simmons, G., R. J. Wool-Lewis, F. Baribaud, R. C. Netter, and P. Bates.** 2002. Ebola virus glycoproteins induce global surface protein down-modulation and loss of cell adherence. J. Virol. **76**:2518–2528.
40. **Simmons, G., J. D. Reeves, C. C. Grogan, L. H. Vandenberghe, F. Baribaud, J. C. Whitbeck, E. Burke, M. J. Buchmeier, E. J. Soilleux, J. L. Riley, R. W. Doms, P. Bates, and S. Pöhlmann.** 2003. DC-SIGN and DC-SIGNR bind Ebola glycoproteins and enhance infection of macrophages and endothelial cells. Virology **305**:115–123.
41. **Slenczka, W. G.** 1999. The Marburg virus outbreak of 1967 and subsequent episodes. Curr. Top. Microbiol. Immunol. **235**:49–75.
42. **Smith, D. H., B. K. Johnson, M. Isaacson, R. Swanapoel, K. M. Johnson, M. Killey, A. Bagshawe, T. Siongok, and W. K. Keruga.** 1982. Marburg-virus disease in Kenya. Lancet **i**:816–820.
43. **Still, W. C., A. Tempczyk, R. C. Hawley, and T. Hendrickson.** 1990. Semianalytical treatment of solvation for molecular mechanics and dynamics. J. Am. Chem. Soc. **112**:6127–6129.
44. **Suzuki, N., K. Yamamoto, S. Toyoshima, T. Osawa, and T. Irimura.** 1996. Molecular cloning and expression of cDNA encoding human macrophage C-type lectin. Its unique carbohydrate binding specificity for Tn antigen. J. Immunol. **156**:128–135.
45. **Takada, A., C. Robison, H. Goto, A. Sanchez, K. G. Murti, M. A. Whitt, and Y. Kawaoka.** 1997. A system for functional analysis of Ebola virus glycoprotein. Proc. Natl. Acad. Sci. U. S. A. **94**:14764–14769.
46. **Takada, A., K. Fujioka, M. Tsuiji, A. Morikawa, N. Higashi, H. Ebihara, D. Kobasa, H. Feldmann, T. Irimura, and Y. Kawaoka.** 2004. Human macrophage C-type lectin specific for galactose and N-acetylgalactosamine promotes filovirus entry. J. Virol. **78**:2943–2947.
47. **Tsui, V., and D. A. Case.** 2000. Theory and applications of the generalized Born solvation model in macromolecular simulations. Biopolymers **56**:275–291.
48. **Volchkov, V. E., A. A. Chepurnov, V. A. Volchkova, V. A. Ternovoj, and H. D. Klenk.** 2000. Molecular characterization of guinea pig-adapted variants of Ebola virus. Virology **277**:147–155.
49. **Wang, S. F., J. C. Huang, Y. M. Lee, S. J. Liu, Y. J. Chan, Y. P. Chau, P. Chong, and Y. M. Chen.** 2008. DC-SIGN mediates avian H5N1 influenza virus infection in cis and in trans. Biochem. Biophys. Res. Commun. **373**: 561–566.
50. **Weissenhorn, W., A. Carfí, K. H. Lee, J. J. Skehel, and D. C. Wiley.** 1998. Crystal structure of the Ebola virus membrane fusion subunit, GP2, from the envelope glycoprotein ectodomain. Mol. Cell **2**:605–616.
51. **Wong, A. C., R. G. Sandesara, N. Mulherkar, S. P. Whelan, and K. Chandran.** 2010. A forward genetic strategy reveals destabilizing mutations in the ebolavirus glycoprotein that alter its protease dependence during cell entry. J. Virol. **84**:163–175.
52. **Yang, Z. Y., H. J. Duckers, N. J. Sullivan, A. Sanchez, E. G. Nabel, and G. J. Nabel.** 2000. Identification of the Ebola virus glycoprotein as the main viral determinant of vascular cell cytotoxicity and injury. Nat. Med. **6**:886–889.
53. **Zhou, T., Y. Chen, L. Hao, and Y. Zhang.** 2006. DC-SIGN and immunoregulation. Cell. Mol. Immunol. **3**:279–283.